European Journal of Operational Research 306 (2023) 189–206

Contents lists available at ScienceDirect

European Journal of Operational Research

journal homepage: www.elsevier.com/locate/ejor

Production, Manufacturing, Transportation and Logistics

An exact approach for the multi-depot electric bus scheduling problem with time windows

K. Gkiotsalitis [a,*], C. Iliopoulou [b], K. Kepaptsoglou [b]

[a] University of Twente, Dept. of Civil Engineering, Transport Engineering and Management, P.O. Box 217, AE Enschede 7500, The Netherlands
[b] School of Rural and Surveying Engineering, National Technical University of Athens, 9, Iroon Polytechniou str, Zografou Campus, 15780, Greece

ARTICLE INFO

Article history:
Received 17 December 2021
Accepted 11 July 2022
Available online 16 July 2022

Keywords:
Transportation
Electric bus scheduling
Charging
MDVSPTW
Exact optimization

ABSTRACT

This study extends the multi-depot vehicle scheduling problem with time windows (MDVSPTW) to the case of electric vehicles which can recharge at charging stations located at any point of the service operation area. We propose a mixed-integer nonlinear model for the electric bus multi-depot vehicle scheduling problem with time windows (EB-MDVSPTW). Our formulation considers not only the operational cost of vehicles, but also the waiting times. In addition, it explicitly considers the capacity of charging stations and prohibits the simultaneous charging of different vehicles at the same charger. Chargers are modeled as task nodes of an extended network and can be placed at any location utilizing the charging infrastructure of a city instead of using only bus-dedicated chargers. Further, we linearize the MINLP formulation of the EB-MDVSPTW by reformulating it to a mixed-integer linear program (MILP) that can be solved to global optimality. Because EB-MDVSPTW is NP-Hard, we also introduce valid inequalities to tighten the search space of the MILP and we investigate the trade-off between the compactness and the tightness of the problem in benchmark instances with up to 30 trips. In the numerical experiments, we show that the valid inequalities reduce the problem's compactness by increasing up to three times the number of constraints, but, at the same time, improve tightness resulting in computational time improvements of up to 73% in 20-trip instances. The implementation of our exact approach is demonstrated in a toy network and in the benchmark instances of Carpaneto et al. (1989).

1. Introduction

Public transport systems are gradually shifting to electromobility as dictated by global environmental mandates which set specific emission reduction targets for urban centers (Wang, Huang, Xu, & Barclay, 2017). Electric bus fleets bring forth a new set of managerial challenges for transit operators. Planning for electric bus systems is a complex task since vehicle energy sufficiency and charging requirements must be taken into account (Iliopoulou, Tassopoulos, Kepaptsoglou, & Beligiannis, 2019). As such, the electrification of public transport calls for new planning models for network design, timetabling and scheduling, under charging infrastructure and energy supply considerations (Häll, Ceder, Ekström, & Quttineh, 2019).

The deployment of electric fleets significantly complicates vehicle scheduling, which is a crucial step in the public transport planning process (Häll et al., 2019). The solution of the associated Vehicle Scheduling Problem (VSP), which entails assigning vehicles to timetabled trips, allows for evaluating the feasibility and cost of the proposed timetable under the available fleet (Desaulniers & Hickman, 2007). An infeasible or undesirable solution for the VSP can lead to a revision of the timetable and even of the route frequencies (Desaulniers & Hickman, 2007). In the case of an electric fleet, scheduling must consider charging activities, apart from vehicle trips. Evidently, the need to incorporate vehicle recharging trips in the current schedule while maintaining the existing level of service introduces a new layer of complexity to the scheduling problem. Furthermore, charging activities for the entire electric bus fleet may be typically performed at a limited set of locations, therefore perplexing scheduling decisions (Gkiotsalitis, 2020).

Reasonably, different vehicle charging technologies introduce distinct methodological intricacies to the VSP and are linked with different modeling needs (Häll et al., 2019). Specifically, the advent of opportunity charging significantly complicates the VSP, compared, for instance, to overnight charging. Opportunity charging systems exploiting wireless power transfer have been deployed in major European and U.S. urban centers over the past few years, achieving high charging efficiency rates

* Corresponding author.
E-mail addresses: k.gkiotsalitis@utwente.nl (K. Gkiotsalitis), christiliop@central.ntua.gr (C. Iliopoulou), kkepap@central.ntua.gr (K. Kepaptsoglou).

https://doi.org/10.1016/j.ejor.2022.07.017

(Iliopoulou & Kepaptsoglou, 2019b). Under this configuration, buses can optionally charge at terminals and intermediate stops exploiting layover and dwell times (Iliopoulou et al., 2019). The necessary input for the VSP in this case includes battery capacity, charger locations and possible charging times, which in turn affect the scheduling constraints and cost components (Häll et al., 2019). What is more, since vehicles charge periodically at bus stops rather than the depot, concerns on reliability and bus bunching phenomena arise (Chioni, Iliopoulou, Milioti, & Kepaptsoglou, 2020; Gkiotsalitis, 2021; Iliopoulou, Milioti, Vlahogianni, & Kepaptsoglou, 2020). Buses' inability to charge upon arrival at a station due to limited charging outlets or stop space can lead to vehicle platooning and queuing delays (Iliopoulou & Kepaptsoglou, 2021). These issues naturally cause increased passenger waiting times and discomfort, adversely affecting the perceived image of public transport services and operators' profitability (Gkiotsalitis, 2019; Gkiotsalitis & Cats, 2020; Iliopoulou et al., 2020).

Therefore, efficient scheduling for electric buses must consider the possibility of overlapping charging activities among different lines to mitigate bus bunching concerns. Furthermore, traffic conditions and unexpected events induce stochasticity in vehicle trip times, calling for flexibility in scheduling models (Gkiotsalitis & Alesiani, 2019; Gkiotsalitis & Cats, 2018; Iliopoulou & Kepaptsoglou, 2019a). Such models may also need to consider the possibility of shared charging among different vehicle fleets. Budget constraints, urban space limitations and high charging demand can render shared charging among heterogeneous transport fleets a prominent option for large-scale urban fleet electrification (Wang et al., 2019). In this configuration, electric buses can charge at publicly or privately owned multi-use electric vehicle charging stations located within their service areas (Esmailirad, Ghiasian, & Rabiee, 2021).

As such, aiming to provide a realistic scheduling model for electric bus systems, this study deals with electric bus scheduling and, in particular, the multi-depot VSP (MDVSP) under time windows and charger scheduling constraints, considering opportunity charging at bus stops, terminal stations and mixed-use electric vehicle charging stations. Allowing trips to start within a specific time interval can capture trip time variability and provide managerial flexibility while improving operational efficiency (Bunte & Kliewer, 2009; Kliewer, Amberg, & Amberg, 2012; Schmid & Ehmke, 2015). Moreover, the consideration of time windows prevents early or delayed arrivals to charging stations and, in conjunction with charger scheduling constraints, can alleviate queuing effects due to shared terminal charging. To the best of the authors' knowledge, no study has so far addressed the multi-depot electric vehicle scheduling under time windows and charger availability constraints. We refer to the problem at hand as Electric Bus Multiple-depot Vehicle Scheduling Problem in Time Windows (EB-MDVSPTW) and present a mixed-integer nonlinear program (MINLP), which is subsequently linearized and solved to global optimality using the branch-and-cut method. The model is first validated on a toy network and then applied to benchmark instances.

The remainder of this paper is structured as follows. The next section presents a literature review on electric bus scheduling models and outlines our contribution. Subsequently, the proposed mathematical models are presented. Results on the toy network as well as benchmark instances and a real-world case are offered and discussed. The paper concludes with findings and remarks for future research.

2. Literature review and contribution

2.1. A brief on the VSP

The VSP generally refers to the assignment of set of timetabled trips to a set of vehicles subject to operational constraints. There are two main categories of VSPs, the single depot VSP (SDVSP) and the MDVSP. The SDVSP arises for small to medium-size transit agencies that rely on a single depot or in the context of decomposing the MDVSP (Desaulniers & Hickman, 2007). The SDVSP is polynomially solvable and can be formulated as a minimum-cost network flow problem, a linear assignment problem, a transportation problem, and a matching problem (Bunte & Kliewer, 2009; Desaulniers & Hickman, 2007). In contrast, the MDVSP is NP-Hard and is typically solved using heuristic and metaheuristic approaches. It has been formulated as a single-commodity network flow model, a multi-commodity network flow model and a set partitioning model (Bunte & Kliewer, 2009; Desaulniers & Hickman, 2007). For a thorough overview of models and solution approaches for the VSP, the interested reader is referred to the reviews by Bunte & Kliewer (2009); Desaulniers & Hickman (2007); Ibarra-Rojas, Delgado, Giesen, & Muñoz (2015) and more recently, Liu & Ceder (2021).

2.2. Electric vehicle scheduling

The wider adoption of electric buses has shifted the research attention towards the electric VSP (E-VSP) and its variants, taking into account the deployment of electric bus fleets and charging infrastructures. The E-VSP is an extension of the VSP, as in this case a set of timetabled trips must be assigned to a set of electric vehicles with limited driving ranges, therefore distance and recharging constraints also apply. Computationally, it has been shown that the E-VSP is NP-Hard (Li, 2014). The E-VSP under various electrification technologies has been tackled both with exact models and metaheuristics. Early models treated range considerations associated with electric fleets through the incorporation of the so-called Route Time Constraints (RTCs) in the VSP, defining a limit on the time vehicles can spend away from the depot (Haghani & Banihashemi, 2002). In this line of work, Wang & Shen (2007) presented one of the first models considering the VSP under limited energy, employing an ant colony algorithm for its solution. In a similar approach, both Zhu & Chen (2013) and Li (2014) formulated the E-VSP under battery swapping as a SDVSP with RTCs, using a Non-dominated Sorting Genetic Algorithm-II (NSGA- II) and a column-generation-based (CG) algorithm, respectively. Overall, this earlier stream of studies sought to design vehicle schedules ensuring energy sufficiency, yet scheduling of charging activities was not explicitly considered.

Over the past few years, a multitude of studies have presented mathematical programming models along with heuristic/metaheuristic solution algorithms for devising schedules for electric buses under various charging configurations, also seeking to optimize other system-related aspects, such as charger location and number, fleet and battery size. A large part of the literature has dealt with multiple aspects of electric fleet management considering a single depot. In this context, Rogge, van der Hurk, Larsen, & Sauer (2018) addressed the E-VSP under depot charging while also optimizing fleet size and charging infrastructure, with the aim of total cost of ownership (TCO) minimization for the electric fleet. The authors used a genetic algorithm (GA) to group trips and a mixed integer programming (MIP) model to determine charger locations. Similarly, Jefferies & Göhlich (2020) aimed to minimize TCO for electric fleets, employing a greedy heuristic to determine vehicle schedules and a GA to optimize opportunity charging locations. Stumpe, Rößler, Schryen, & Kliewer (2021) employed a Variable Neighborhood Search-based algorithm to simultaneously determine the charging infrastructure and schedules for an electric fleet housed at a single depot. In a similar approach, Jovanovic, Bayram, Bayhan, & Voß (2021) presented a greedy randomized adaptive search procedure (GRASP) algorithm for handling large-scale instances under depot charging with the objective

of fleet size minimization. Alvo, Angulo, & Klapp (2021) used Benders' decomposition to solve the 'master' vehicle scheduling problem and the 'satellite' problem of sequencing charging tasks. Recently, Perumal et al. (2021a) presented an adaptive large neighborhood search (ALNS) along with branch-and-price heuristics for the integrated single-depot E-VSP and crew scheduling problem, considering labor regulations for the crew while minimizing total operational cost.

Several studies have attempted to more realistically model the E-VSP through the integration of stochastic effects. Tang, Lin, & He (2019) dealt with electric bus scheduling with limited capacity for the single-depot case and developed both static and dynamic models that took into account uncertainty related to traffic conditions. The proposed mixed integer linear programming (MILP) models were solved using a branch-and-price framework. Bie, Ji, Wang, & Qu (2021) took into account both trip time and energy consumption uncertainty in the E-VSP, proposing a NSGA-II approach to solve the problem. Another stream of studies incorporated concerns related to battery degradation in the E-VSP. Taking into account electricity price and battery depth-of-discharge, van Kooten Niekerk, Van den Akker, & Hoogeveen (2017) proposed two mathematical programming models to account for different charging processes. For small/medium instances the models were solved using CPLEX, while CG and Lagrangian relaxation were employed for larger instances. Wang, Kang, & Liu (2020) formulated the electric bus fleet scheduling problem under battery capacity fading as a multi-stage decision-making problem, employing dynamic programming to minimize battery replacement costs. Similarly, Zhang, Wang, & Qu (2021b) modeled the E-VSP as a set partitioning model and applied a branch-and-price approach to determine vehicle schedules while taking battery health into account.

As a way to mitigate energy sufficiency concerns, a few studies studied the E-VSP in the case of dynamic wireless power transfer (DWPT). This technology allows buses to charge while driving, therefore reducing reliance on stationary charging (Iliopoulou & Kepaptsoglou, 2019b). In this line of research, Alwesabi, Wang, Avalos, & Liu (2020) developed an integer programming model for electric bus and fleet sizing under DWPT. Similarly, Yıldırım & Yıldız (2021) investigated the electric bus fleet composition multi-depot scheduling problem under a combination of static charging and DWPT, proposing an efficient CG-based algorithm.

In the recent years, several researchers have also investigated the MDVSP in the context of electric fleets, formulating the so-called MD-E-VSP. Liu & Ceder (2020) proposed a model based on deficit function theory as well as a mathematical programming model to determine schedules for electric fleets under optimal number of fast-chargers and partial charging. Li et al. (2020) determined the optimal assignment of trips to vehicles and the allocation of battery chargers to charging stations, minimizing the total investment cost of the transit system. The associated problem was solved with an adaptive GA. Wen, Linde, Ropke, Mirchandani, & Larsen (2016) presented a MIP model for the MD-E-VSP with time windows under partial charging. The problem was solved using CPLEX for smaller instances and an ALNS algorithm for larger instances. A similar MD-E-VSP model was adopted by Wang, Guo, & Zuo (2021) who employed a GA-based CG approach to efficiently solve it.

The aforementioned studies have considered fully electric homogeneous vehicle fleets. Still, in some cases operators opt for gradual fleet electrification, introducing electric vehicles in a subset of lines at first (Pylarinou, Iliopoulou, & Kepaptsoglou, 2021). In one of the earlier studies presenting scheduling tools for mixed fleets, Paul & Yamada (2014) utilized a greedy algorithm for scheduling of electric buses and conventional buses, performing simulations using real bus data to evaluate generated solutions. Li, Lo, & Xiao (2019) formulated the MDVSP with multiple vehicle types (electric and conventional) as an integer linear program, simultaneously optimizing the location of refueling stops. Lu, Yao, Zhang, & Yang (2021) presented a MDVSP model and a GA for mixed-fleet scheduling, incorporating the concept of trip buffer time to mitigate driving time uncertainty effects. Considering a single depot, Zhou, Xie, Zhao, & Lu (2020) formulated the SDVSP for a mixed fleet of both conventional and electric transit buses as a bi-level model and solved it using a hybrid iterative neighborhood search algorithm. In a similar context, Rinaldi, Picarelli, D'Ariano, & Viti (2020) presented a MILP model for optimal scheduling of a mixed fleet of electric and hybrid buses along with an ad-hoc decomposition scheme to improve the scalability of the proposed model.Some studies incorporated bus fleet heterogeneity in the E-VSP through the consideration of multiple types of electric buses featuring different passenger and battery capacities. Yao, Liu, Lu, & Yang (2020) developed a GA-based heuristic procedure for solving the MD-E-VSP with multiple vehicle types, minimizing initial investment and operating costs. Similarly, the MD-E-VSP under a heterogeneous electric fleet was addressed by Zhang et al. (2021a), who developed a MIP model and used an ALNS algorithm to handle the problem's complexity.

Of relevance to this stream of studies are also studies dealing with optimal fleet management for transition to electric buses (Pelletier, Jabali, Mendoza, & Laporte, 2019) as well as studies dealing with joint fleet management and infrastructure location decisions (An, 2020; Guschinsky, Kovalyov, Rozin, & Brauner, 2021). For a thorough review on electric bus planning models and corresponding solution approaches, the interested reader is referred to the study by Perumal, Lusby, & Larsen (2021b).

2.3. Charging scheduling for electric vehicles

A branch of the relevant literature has exclusively focused on optimizing charging schedules, treating vehicle schedules as predetermined inputs. Such studies have presented MILP models which could be solved by off-the-shelf commercial solvers like CPLEX. In this context, Wang et al. (2017) determined optimal charging schedules and charging infrastructure for electric bus fleets. He, Liu, & Song (2020) and Liu, Gao, Liang, Zhao, & Li (2021) investigated both optimal charging scheduling and charging power management for fast-charging electric bus systems. Abdelwahed, van den Berg, Brandt, Collins, & Ketter (2020) proposed a MILP model for charging schedule optimization under opportunity charging, aiming to minimize charging costs and grid impacts. Another branch of the relevant literature has exploited simulation to evaluate charging schedules for electric buses. Such studies combine simulation and real-world data to evaluate various charging strategies and infrastructure configurations for bus networks taking into account demand charges (Qin, Gusrialdi, Brooker, Ali et al., 2016), operating and construction costs (Ke, Chung, & Chen, 2016; Mohamed, Farag, El-Taweel, & Ferguson, 2017; Teoh, Khoo, Goh, & Chong, 2018) as well as battery-related decisions (Gao et al., 2017).

2.4. Contribution

The overview of the literature underlines the increasing research interest for the E-VSP and its variants. The literature on the MD-E-VSP is summarized in Table 1, which presents the problem characteristics and solution approaches.

In general, relatively few studies have dealt with the MD-E-VSP (Wang et al., 2021), relying on metaheuristics to solve larger instances of the problem (Li et al., 2020; Wang et al., 2021; Wen et al., 2016). Furthermore, existing studies have scarcely considered the option of time windows for trips and charging tasks.

Table 1
Literature summary.

Reference	Fully electric fleet	Charging location	Recharging type	Time-windows	Charger scheduling constraints	Waiting cost minimization	Solution approach
Wen et al. (2016)	✓	Charging stations	Partial	✓			MIP/ALNS
Li et al. (2019)		Charging stations	Fixed duration, once per bus		✓	✓	Integer linear Programming
Liu & Ceder (2020)	✓	Terminal stations	Full/partial				Heuristic
Li et al. (2020)	✓	Subset of terminal stations	Partial		✓		Adaptive GA
Yao et al. (2020)	✓ (heterogeneous)	Charging stations at depots	Full				GA-based heuristic
Yıldırım & Yıldız (2021)		Charging stations at depots and DWPT	Partial				CG-based algorithm
Wang et al. (2021)	✓	Charging stations	Full			✓	GA-based CG approach
Lu et al. (2021)		Charging stations at depots	Full	✓ (trip buffer time)	✓		GA
Zhang et al. (2021a)	✓ (heterogeneous)	Charging stations at depots	Partial				ALNS
This study	✓	Charging stations	Full	✓	✓	✓	MILP

Only Wen et al. (2016) presented a model for the MD-E-VSP under partial charging and solved it using an ALNS approach for instances over 30 trips. However, charger availability was not considered in this study, overlooking the possibility of queue formation at stops. In general, the literature on electric vehicle scheduling has so far mostly focused on vehicles, neglecting charger scheduling considerations (Li et al., 2020). In fact, although queuing has been modeled within relevant simulation frameworks (Mohamed et al., 2017), studies optimizing vehicle charging schedules have typically adopted simplifying assumptions, such as the lack of queues at terminal stations (He et al., 2020). Only a few exceptions may be noted. Li et al. (2019) took refueling station capacity into account, presenting a linear formulation for the mixed-fleet MDVSP, yet employed simplifying assumptions constraining the number of refueling trips to one per vehicle during operation. Recently, Li et al. (2020) concurrently addressed vehicle and charger scheduling in the MD-E-VSP, which they tackled using an adaptive GA, yet did not consider time windows or full recharging. To the authors' knowledge, there is no study that simultaneously considers the MD-E-VSP under time windows, charger scheduling constraints and full recharging, while also employing an exact solution approach. As such, this study makes the following contributions:

- We extend the multi-depot vehicle scheduling problem with time windows (MDVSPTW) proposed by Desaulniers, Lavigne, & Soumis (1998) to the case of electric bus systems under full recharging at charging stations which can be located at any point of the service operation area (EB-MDVSPTW).
- We propose a mixed-integer linear program (MILP) that can be solved to global optimality for the EB-MDVSPTW. The model not only considers the operational cost of buses, but also the vehicle waiting time.
- We explicitly consider charging station capacity and prohibit simultaneous charging of different buses at the same charger.
- We introduce valid inequalities to tighten the solution space and analyze the trade-off between the increase of the size of the problem and the reduction of the computational complexity.

3. Problem description

3.1. Short description of MDVSPTW

The problem description of the EB-MDVSPTW problem expands the problem description of the Multiple-depot Vehicle Scheduling Problem in Time Windows (MDVSPTW). In the MDVSPTW: (1) every trip has to be assigned to exactly one vehicle; (2) every vehicle is associated with a single depot; (3) each vehicle starts from the depot and returns to it only once, e.g., at the end of its daily schedule; and (4) the starting and end times of trips are not fixed, but they can take values within a time range (time window). Note that this is particularly important when accounting for travel time uncertainty.

We briefly introduce the MDVSPTW formulation of Desaulniers et al. (1998) which is extended in this study. MDVSPTW seeks to find the minimum cost exact cover of all scheduled trips during the daily operations. The main assumption is that each vehicle starts from its depot and it will return to it just once. The MDSVSPTW is a discrete optimization problem with a combinatorial origin. Formally, let K be a set of available vehicles and $G^k = (V^k, A^k)$ the network associated with vehicle k, where V^k are the nodes and A^k the arcs. The source and sink nodes associated with the depot housing vehicle k are denoted as o_k and d_k, respectively. These nodes indicate the start and the end of the schedule assigned to vehicle $k \in K$. In our network representation, each node corresponds to a *scheduled trip* with a specific start and end stop and each arc indicates the *transfer* of a vehicle from one trip to another one.

The set of all possible task nodes is N, where task $i \in N$ corresponds to a scheduled trip with a specific start and end stop that needs to be served by a vehicle $k \in K$. In addition, each node $i \in N$ is associated with a time window $[l_i, u_i]$ indicating the time period within which we should perform task i. We have also a set of *empty, start, end* and *inter-task* arcs A^k. Arc (o_k, i), where $i \in V^k$, is a start arc. Arc (i, d_k) is an end arc, arc (o_k, d_k) is an empty arc, and arc (i, j), where $i \in V^k \setminus \{o_k, d_k\}$ and $j \in V^k \setminus \{o_k, d_k\}$, is an inter-task arc. The elapsed time on arc (i, j) that connects nodes i and j is denoted as t_{ij}. This time is equal to the duration of task i plus the travel time between the end location of task i and the start location of task j. Clearly, $t_{o_k,d_k} = 0$. It is also worth noting that this elapsed time is not vehicle-specific. A vehicle incurs waiting costs if it needs to wait between two successive tasks, i.e. when the difference between the start times of the two tasks is greater than the time needed to complete the first task plus the time required to travel between its end location and the start location of the second task. The corresponding delay is multiplied by the unit waiting cost of a vehicle, which is denoted by λ, to estimate the associated waiting costs. We have an indicator parameter I^k_{ij}, where $I^k_{ij} = 1$ if (i, j) is an *inter-task* arc and 0 otherwise. Finally, the cost constant component of performing task j after task i without considering

any potential delay (task j starts immediately after i without time delays) is b_{ij}^k.

The variables of the MDVSPTW problem are:

x_{ij}^k : binary flow variable, where $x_{ij}^k = 1$ if vehicle k uses arc (i, j) and 0 otherwise.

T_i^k : a time variable associated with each node $i \in V^k$. $T_{o_k}^k$ indicates the departure time from the depot, $T_{d_k}^k$ the arrival time at the depot, and T_i^k with $i \in V^k$ the time that service begins at node i.

c_{ij}^k : cost of performing task j immediately after performing task i. For instance, $c_{o_k,j}^k$ is the cost of performing task j after starting from the depot and c_{i,d_k}^k is the cost of returning to the depot after performing task i.

The cost of performing task j immediately after task i by vehicle k is:

$$c_{ij}^k = b_{ij}^k + I_{ij}^k \lambda \left(T_j^k - T_i^k - t_{ij}\right)$$

where the waiting cost $I_{ij}^k \lambda (T_j^k - T_i^k - t_{ij})$ is added to the cost constant component b_{ij}^k of performing task j after task i without considering any potential delay. The MDVSPTW can be formulated as the following mixed-integer nonlinear multi-commodity network flow model:

$$\min \sum_{k \in K} \sum_{(i,j) \in A_k} \left(b_{ij}^k + I_{ij}^k \lambda \left(T_j^k - T_i^k - t_{ij}\right)\right) x_{ij}^k \tag{1}$$

$$\text{subject to: } \sum_{k \in K} \sum_{j:(i,j) \in A_k} x_{ij}^k = 1 \qquad \forall i \in N \tag{2}$$

$$\sum_{j:(o_k,j) \in A^k} x_{o_k,j}^k = \sum_{i:(i,d_k) \in A^k} x_{i,d_k}^k = 1 \qquad \forall k \in K \tag{3}$$

$$\sum_{i:(i,j) \in A^k} x_{ij}^k - \sum_{i:(j,i) \in A^k} x_{ji}^k = 0 \qquad \forall k \in K \ \forall j \in N \tag{4}$$

$$x_{ij}^k (T_i^k + t_{ij}) \leq x_{ij}^k T_j^k \qquad \forall k \in K \ \forall (i,j) \in A^k \tag{5}$$

$$l_i \leq T_i^k \leq u_i \qquad \forall k \in K \ \forall i \in V^k \tag{6}$$

$$x_{ij}^k \in \{0, 1\} \qquad \forall k \in K \ \forall (i,j) \in A^k \tag{7}$$

where the objective function is nonlinear and seeks to minimize the total cost, including potential delays when waiting between activities i and j.

3.2. Extension to the EB-MDVSPTW problem

In this study we expand the Multiple-depot Vehicle Scheduling Problem in Time Windows to the case of electric buses. In the MDVSPTW case, each vehicle k started from its depot and returned to the same depot at the end of its daily schedule. When considering charging, EBs have to visit the location of charging stations if their State of Charge (SOC) is low. The charging stations can be located at any point in the network, even at the locations of depots. Some of them might be placed at the same location. We consider a set of $Z = \{1, \ldots, z, \ldots, |Z|\}$ charging stations in our bus network. Charging can be seen as an additional task, but, unlike tasks that refer to pre-scheduled trips, the number of charging requests per charging station is not fixed because it depends on the fleet scheduling.

In EB-MDVSPTW we adopt the assumptions of the MDVSPTW and we introduce the following additional ones: (1) all EBs are fully charged at the beginning of the day; (2) charging infrastructure can be shared among different EBs, but two EBs cannot use the same charger simultaneously; (3) all installed chargers have the same charging supply rate; and (4) EBs recharge fully when plugged in a charging station.

Let F be the set of all possible charging events. Each possible charging event $i \in F$ can start within the time window $[l_i, u_i]$. Charging events $i \in F$ associated with charger $z \in Z$ form a subset $F^z \subseteq F$. Each possible charging event $i \in F$ can be seen as an additional node in the network of a vehicle $k \in K$ that comprises the following nodes:

$$N^k = \{V^k \cup F \cup \{o_k, d_k\}\}$$

where $V^k \subseteq V$ are the trips that can be potentially performed by vehicle k and are a subset of set V denoting all trips, (o_k, d_k) the origin and destination depots of trip k, and F the set of all charging events. The set of all nodes that are available to all vehicles is:

$$N = \{V \cup F \cup O \cup D\}$$

where O and D are the sets of the origin and destination depots for all vehicles. It follows that $N^k \subseteq N$.

Network G^k is now expanded to:

$$G^k = (N^k, A^k)$$

We note that G^k is vehicle-dependent and, in the extreme case of no vehicle-related restrictions ($N^k = N$), it can coincide with the complete network. The set of arcs A^k is now expanded and it is the union of the following arcs:

$$A^k = \begin{cases} A_1^k = (o_k, j) & \forall j \in N^k - \{o_k\} \\ A_2^k = (j, d_k) & \forall j \in N^k - \{o_k, d_k\} \\ A_3^k = (i, j) & \forall i \in V^k \ \ \forall j \in V^k - \{i\} \\ A_4^k = (i, j) & \forall i \in V^k \ \ \forall j \in F \\ A_5^k = (i, j) & \forall i \in F \ \ \forall j \in V^k \end{cases}$$

For vehicle $k \in K$, arcs A_1^k are all feasible arcs that start from the origin depot, A_2^k are all feasible arcs that connect a node to the destination depot, A_3^k are all feasible arcs which represent the traveling from the end location of trip $i \in V^k$ to the start location of trip $j \in V^k - \{i\}$, A_4^k are all feasible arcs which represent the traveling from the end location of trip i to the location of the charging event $j \in F$, and arcs A_5^k are all feasible arcs which represent the traveling from the location of charging event $i \in F$ to the start location of trip j. The network G^k of a vehicle k with two trip task nodes and two charging event task nodes is illustrated in Fig. 1. In the left part of the figure we present the physical locations of the origin and destination depots, o_k, d_k, the trips that can be potentially performed by vehicle k, $V^k = \{1, 2\}$, and the charger z that can accommodate two charging events $F = \{a, b\}$. Note that the two trips serve 3 stops and they operate at the same line. In addition, the two charging events are at the same charger. In the right part of the figure we translate the physical network to the modeled network representation $G^k = \{N^k, A^k\}$. We first create the task nodes $N^k = \{V^k \cup F \cup \{o_k, d_k\}\}$, where $V^k = \{1, 2\}$ representing the two trip tasks and $F = \{a, b\}$ representing the two charging event tasks. Note that even if the trips operate at the same line and the charging events are at the same charger, we represent them in the graph as independent nodes without using information about their physical location. In other words, the modeled network is an abstract construct that does not use the actual coordinates of task nodes in this visualization. After visualizing the task nodes, we generate the arcs A^k such that arcs can go from the origin depot o_k to any other task node except o_k, d_k, from any

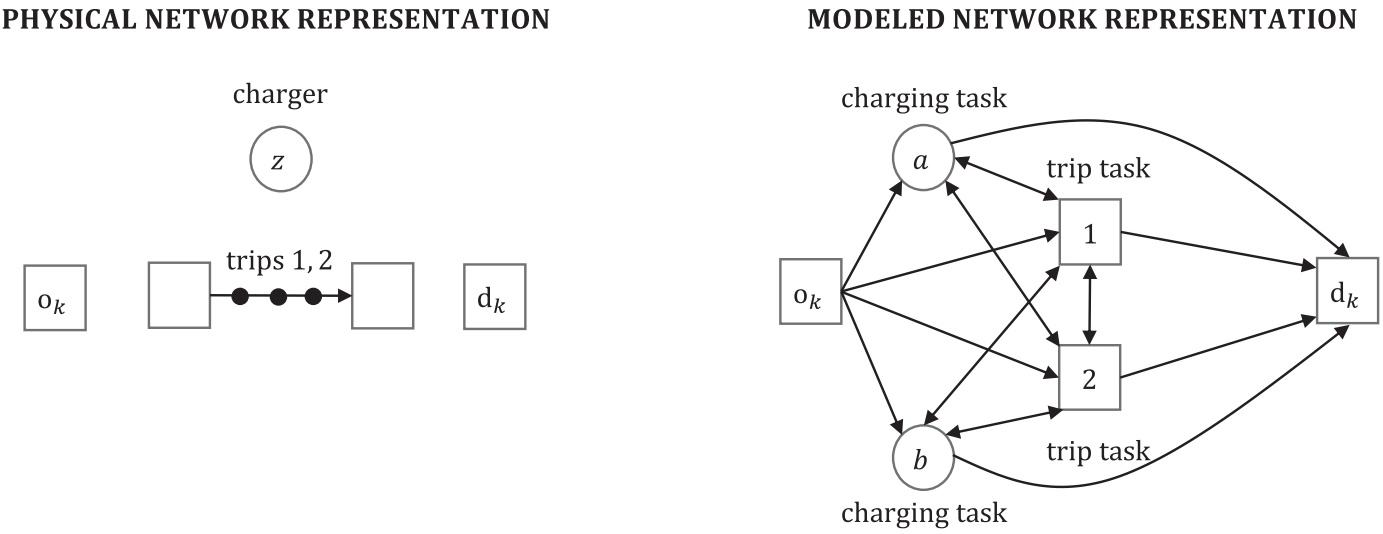

Fig. 1. Physical vs Modeled representation of the network $G^k = \{N^k, A^k\}$ of a vehicle k.

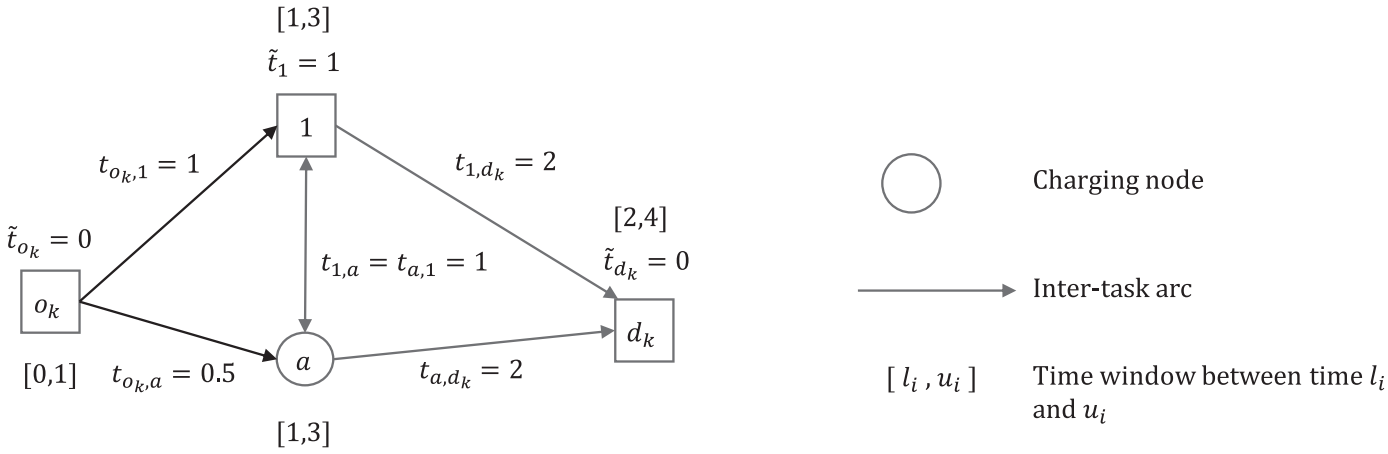

Fig. 2. Example of inter/intra-task travel times, and time windows.

task node $i \in V^k$ to any other task node $j \in V^k \cup F - \{i\}$, from any task node $i \in F$ to any other task node $j \in V^k$, and from any task node $j \in N^k - \{o_k, d_k\}$ to the destination depot d_k. Note that arcs that connect directly charging tasks $F = \{a, b\}$ are not permitted.

Every node has a vehicle-independent lower and upped time bound of starting the task associated with it. This is expressed by $[l_i, u_i]$, where l_i is the lower bound and u_i is the upper bound of every node $i \in N$. In addition, to complete any trip $i \in V$ there is an associated time cost $\tilde{t}_i$, $\forall i \in V$. We note that the time window to perform a trip is strict (e.g., a trip's starting time cannot be moved from an off-peak time period to a peak time given its time window restrictions) and this does not allow its travel time to change significantly from its estimated value. Thus, $\tilde{t}_i$ is considered as a parameter. To travel from the end location of the task at node $i \in N$ to the start location of the task at node $j \in N$ there is an associated travel cost t_{ij}. Note that the end and start location of any depot node $i \in O \cup D$ is the same because we do not perform a deadheading when staying at the depot. The same is true for any charging event node $i \in F$. If, however, node i is a trip, e.g., $i \in V$, then t_{ij} is the travel time to deadhead from the end location of trip i to the start location of j. Consider, for instance, the representation of Fig. 2 which describes the time windows $[l_i, u_i]$ at each task node $i \in \{o_k, 1, a, d_k\}$ of a vehicle k, where 1 is a trip task and a a charging event task. Note that each arc has an associated travel time, i.e., $t_{1,a} = 1$ means that the travel time from task 1 to task a is equal to one. If vehicle k starts from depot o_k at time 0 it can arrive and start its service at task 1 at time $T_1^k = \tilde{t}_{o_k} + t_{o_k,1} = 1$. Proceeding to charging task a will need an additional time $\tilde{t}_1 + t_{1,a} = 1 + 1 = 2$ since there is an intra-task travel time cost of $\tilde{t}_1 = 1$ to complete trip 1. Note that, given the time window of each task, the only feasible solution time-wise is the solution of serving tasks $o_k \rightarrow 1 \rightarrow d_k$.

The nomenclature of the EB-MDVSPTW problem is provided in Table 2.

Each vehicle $k \in K$ starts its daily operations fully charged with a SOC $\phi^k_{\max}$. Assuming that all chargers $z \in Z$ have the same charging rate, r, and vehicle k arrives at charging node $i \in F$ at time T_i^k with a current energy level of e_i^k, it will require a time period

$$\tau_i^k = \left(\phi^k_{max} - e_i^k\right)/r$$

to fully recharge. That is, vehicle k can move to the next node after time $T_i^k + \tau_i^k$. Evidently, this computation is based on the assumption that the energy recharged during a charging event is proportional to its duration, i.e. that the charging process is linear. This assumption is widely used for inductive charging of electric vehi-

Table 2
EB-MDVSPTW Nomenclature.

Sets:	
K	set of available vehicles
Z	set of charging stations
O, D	sets of origin and destination depots
V	set of trips
V^k	subset of scheduled trips that can be accomplished by vehicle k
F	set of all possible charging events
F_0	$F_0 \subseteq F$ is the set of all possible charging events after removing the latest possible charging event at every charger
F^z	subset of possible charging events at charger $z \in Z$ ordered from the first to the last
N^k	subset of nodes associated with vehicle k, $V^k \cup F \cup \{o_k, d_k\}$
N	set of all possible task nodes, $N = \{V \cup F \cup O \cup D\}$
A^k	set of feasible arcs for vehicle $k \in K$
G^k	$G^k = (N^k, A^k)$ is the network associated with vehicle k
Parameters:	
o_k, d_k	the source node and the sink node associated with the depot housing vehicle k
$[l_i, u_i]$	time window associated with each node $i \in N$
$t_{i,j}$	elapsed time on arc (i, j) which is equal to the travel time between the end location of task $i \in N$ and the start location of task $j \in N$
$\tilde{t}_i$	required travel time to conduct trip $i \in V$
λ :	unit waiting cost of a vehicle
b^k_{ij}	the cost constant component of performing task j after task i without considering any potential delay (task j starts immediately after i without time delays).
$\phi^k_{\max}$	SOC of vehicle k when it is fully charged
$\phi^k_{\min}$	minimum allowed SOC level for vehicle k
r	charger charging rate
η_i	consumed energy when performing trip $i \in V$
θ_{ij}	consumed energy when deadheading from the end location of node $i \in N$ to the start location of node $j \in N$
M	a very large positive number
q_j	vector $q : V \rightarrow F$ returns the closest charging event location $q_j \in F$ to the end location of trip $j \in V$
ω_i	vector that returns the next charging event of charging event i that is performed at the same charging station
Variables:	
e^k_i	SOC of vehicle k when it arrives at node $i \in V^k \cup F \cup \{d_k\}$
$\bar{e}^k_i$	SOC of vehicle k when it completes the task at node $i \in V^k \cup F \cup \{o_k\}$
τ^k_i	required time period to recharge vehicle k via charging event $i \in F$
g^k_i	vehicle SOC change when performing task $i \in V^k \cup F$
x^k_{ij}	binary flow variables, where $x^k_{ij} = 1$ if vehicle k uses arc $(i, j) \in A_k$ and 0 otherwise
y^k_i	binary indicator variables, where $y^k_i = 1$ if charging event $i \in F$ is performed by trip k and 0 otherwise
T^k_i	time that service begins at node $i \in N^k$. $T^k_{o_k}$ indicates the departure time from the depot, $T^k_{d_k}$ the arrival time at the depot, and T^k_i the time that service begins at any other node $i \in V^k \cup F$

cles, as the battery SOC linearly changes within the minimum and maximum SOC limits (Ko & Jang, 2013).

As previously stated, the SOC of every vehicle k at the beginning of the day is the maximum possible. That is, $\bar{e}^k_{o_k} = \phi^k_{\max}$, where $\bar{e}^k_{o_k}$ is the SOC of vehicle k when departing from node o_k. Given the SOC when vehicle k arrives at node $i \in V^k \cup F$, e^k_i, and when it completes its task at that node, $\bar{e}^k_i$, we have that:

$$\bar{e}^k_i = e^k_i - g^k_i$$

where g^k_i is the vehicle's SOC change when performing task i. If task $i \in V^k$, then vehicle k performs trip i and it consumes energy $\eta_i \geq 0$, which is a pre-determined parameter that depends on the geographical route, number of stops, and terrain profile of the route related to trip i. This is a typical assumption in the literature on electric bus planning (e.g. Kunith, Mendelevitch, & Goehlich (2017); Rogge et al. (2018); Rogge, Wollny, & Sauer (2015)). If, however, $i \in F$, then $g^k_i = e^k_i - \phi^k_{\max}$ because the vehicle will recharge up to its maximum allowed SOC. In the former case, $g^k_i = \eta_i \geq 0$ indicating a SOC reduction, and in the latter case $g^k_i \leq 0$ indicating a SOC increase.

The **vehicle scheduling constraints** are now reformulated as follows:

$$\sum_{k \in K} \sum_{i:(i,j) \in A_k} x^k_{ij} = 1 \qquad \forall j \in V \tag{8}$$

$$\sum_{k \in K} \sum_{i:(i,j) \in A_k} x^k_{ij} \leq 1 \qquad \forall j \in F \tag{9}$$

$$\sum_{j:(o_k,j) \in A^k} x^k_{o_k,j} = \sum_{i:(i,d_k) \in A^k} x^k_{i,d_k} = 1 \qquad \forall k \in K \tag{10}$$

$$\sum_{i:(i,j) \in A^k} x^k_{ij} - \sum_{i:(j,i) \in A^k} x^k_{ji} = 0 \qquad \forall k \in K \ \forall j \in V^k \cup F \tag{11}$$

$$x^k_{ij}\left(T^k_i + \tilde{t}_i + t_{ij}\right) \leq x^k_{ij} T^k_j \qquad \forall k \in K \ \forall (i,j) \in A^k \mid i \in V^k \tag{12}$$

$$x^k_{o_k j}\left(T^k_{o_k} + t_{o_k j}\right) \leq x^k_{o_k j} T^k_j \qquad \forall k \in K \ \forall (o_k, j) \in A^k \tag{13}$$

$$x^k_{ij}\left(T^k_i + \tau^k_i + t_{ij}\right) \leq x^k_{ij} T^k_j \qquad \forall k \in K \ \forall (i,j) \in A^k \mid i \in F \tag{14}$$

$$\tau^k_i = \left(\phi^k_{max} - e^k_i\right)/r \qquad \forall i \in F \ \forall k \in K \tag{15}$$

$$l_i \leq T^k_i \leq u_i \qquad \forall k \in K \ \forall i \in N^k \tag{16}$$

$$x^k_{ij} \in \{0, 1\} \qquad \forall k \in K \ \forall (i,j) \in A^k \tag{17}$$

These constraints include several amendments compared to the MDVSPTW formulation. Constraints (8) ensure that each trip $j \in V$ will be performed by exactly one vehicle. Constraints (9) ensure that a charging event $j \in F$ can be utilized by at most one vehicle. Constraints (10) ensure that each vehicle $k \in K$ will start from

its origin depot and return to its destination depot. Constraints (11) consider the charging events in the network's constraints related to the conservation of flow. Importantly, constraints (12) do not consider arcs that have nodes from set F as their origin nodes because the elapsed travel time between activities (i, j) does not depend on t_{ij}. We introduce constraints (14) where i is a charging event $i \in F$ and the elapsed time on arc (i, j) is equal to the duration of task i, τ_i^k, plus the travel time between the end location of task i and the start location of task j, $\tilde{t}_{ij}$. Constraints (15) return the values of τ_i^k.

In addition to the vehicle scheduling constraints, we have the additional electric charging constraints related to the charging scheduling and the state of charge of EBs. Operating arc $(i, j) \in A^k$ is permitted if, and only if,

$$e_j^k \geq \phi_{min}^k$$

where $e_j^k \geq \phi_{\min}^k$ ensures that the SOC of vehicle k is sufficient when arriving at node j. The **electric charging constraints** are:

$$\tilde{e}_{o_k}^k = \phi_{max}^k \qquad \forall k \in K \tag{18}$$

$$\tilde{e}_j^k = e_j^k - g_j^k \qquad \forall j \in V^k \cup F,\ \forall k \in K \tag{19}$$

$$e_j^k \geq (\tilde{e}_i^k - \theta_{ij}) x_{ij}^k \qquad \forall (i, j) \in A^k,\ \forall k \in K \tag{20}$$

$$e_j^k \leq \left(\tilde{e}_i^k - \theta_{ij}\right) + \left(1 - x_{ij}^k\right) M \qquad \forall (i, j) \in A^k,\ \forall k \in K \tag{21}$$

$$g_i^k = \eta_i \qquad \forall i \in V^k\ \forall k \in K \tag{22}$$

$$g_i^k = e_i^k - \phi_{max}^k \qquad \forall i \in F\ \forall k \in K \tag{23}$$

$$\phi_{min}^k \leq e_j^k \qquad \forall k \in K\ \forall i \in V^k \cup F \cup \{d_k\} \tag{24}$$

$$y_i^k = \sum_{j:(i,j)\in A_k} x_{ij}^k \qquad \forall i \in F\ \forall k \in K \tag{25}$$

$$\sum_{k\in K} y_i^k \left(T_i^k + \tau_i^k\right) \leq T_{\omega_i}^k + M\left(1 - \sum_{\rho:(\omega_i,\rho)\in A^k} x_{\omega_i\rho}^k\right) \qquad \forall i \in F_0,\ \forall k \in K \tag{26}$$

Constraints (18)-(23) return the SOC values when vehicles are traveling between nodes. Notice that when $x_{ij}^k = 1$ constraints (20) and (21) force e_j^k to be equal to the SOC value after departing from node i, $\tilde{e}_i^k$, minus the consumed energy to travel from i to j, θ_{ij}. In more detail, if arc $(i, j) \in A^k$ is not operated by vehicle k then $x_{ij}^0 = 0$ and e_j^k can freely take any value in the range $[0, (\tilde{e}_i^k - \theta_{ij}) + M]$. For a very large number $M \to +\infty$, $e_j^k \in [0, +\infty)$. If, however, $x_{i,j}^k = 1$, then constraint (20) will result in $e_j^k \geq \tilde{e}_i^k - \theta_{ij}$ and constraint (21) will result in $e_j^k \leq \tilde{e}_i^k - \theta_{ij}$ enforcing that $e_j^k = \tilde{e}_i^k - \theta_{ij}$.

Constraints (24) ensure that the SOC of vehicle k when arriving at node $j \in V^k \cup F \cup \{d_k\}$ is greater than or equal to the minimum allowed SOC limit. Finally, constraints (25)-(26) ensure that if a charger $z \in Z$ is used by a vehicle during charging event $i \in F$, the next charging event at the same charger, denoted as ω_i, will start after the end time of the previous charging event. This does not allow two vehicles to use the same single-outlet charger simultaneously. This is made explicit in the following proposition. In more detail, if a charger is used by one vehicle $k \in K$ during charging event $i \in F_0$, then constraints (26) will force y_i^k to be equal to 1. Reckon that from constraints (9) a charging event $i \in F_0$ can be utilized by at most one vehicle, thus the charger $f_i \in Z$ of charging event $i \in F_0$ can be used simultaneously by more than one vehicle if, and only if, the next charging event at the same charger, ω_i, starts before the previous charging event, i, is finished. Let $T_{\omega_i}^k$ be the potential starting time of charging event ω_i for all vehicles $k \in K$. If vehicle $k \in K$ does not utilize charging event ω_i, then $\sum_{\rho:(\omega_i,\rho)\in A^k} x_{\omega_i\rho}^k = 0$ and constraint (26) is satisfied because the right-hand side of the equation approaches $+\infty$. If, however, vehicle $k \in K$ utilizes charging event ω_i that follows charging event i at the same charger, then $\sum_{\rho:(\omega_i,\rho)\in A^k} x_{\omega_i\rho}^k = 1$ and constraint (26) will enforce that $T_{\omega_i}^k \geq \sum_{k\in K} y_i^k (T_i^k + \tau_i^k)$ not allowing the same charger to be used by more than one vehicle at the same time. Finally, if charging event $i \in F_0$ was not used by any vehicle, then the left hand-side of constraint (26) is equal to 0 because $y_i^k = 0$ for all $k \in K$ and the inequality of constraint (26) is satisfied given that the right-hand side of the inequality constraint is always non-negative.

Summarizing, the inequality constraint (26) is satisfied by default if charging event i is not used by any vehicle and if the following charging event at the same charger, ω_i, is not used by a vehicle $k \in K$. If, however, charging event i was used by a vehicle and there is a vehicle $k \in K$ that used charging event ω_i, then the starting time $T_{\omega_i}^k$ is forced to be greater than or equal to the end time of the vehicle that used charging event i, denoted as $\sum_{k\in K} y_i^k (T_i^k + \tau_i^k)$.

The EB-MDVSPTW is formally cast as:

$$\min \sum_{k\in K} \sum_{(i,j)\in A_k \mid i\in V^k} \left(b_{ij}^k + \lambda\left(T_j^k - T_i^k - \tilde{t}_i - t_{ij}\right)\right) x_{ij}^k + \sum_{k\in K} \sum_{(i,j)\in A_k \mid i\in F} \left(b_{ij}^k + \lambda\left(T_j^k - T_i^k - \tau_i^k - t_{ij}\right)\right) x_{ij}^k \tag{27}$$

$$\text{s.t.: vehicle scheduling constraints (8)-(17)} \tag{28}$$

$$\text{electric charging constraints (18)-(26)} \tag{29}$$

The EB-MDVSPTW is a mixed-integer nonlinear program (MINLP) with nonlinear objective function and nonlinear constraints (12),(13),(14),(20),(26). That is, even if we relax the integralities of the binary variables, we still need to solve a nonlinear program with several nonlinear constraints that might prohibit finding a globally optimal solution.

3.3. A note on modeling charging events

In the previous section we considered the general case where each charger $z \in Z$ has a number of charging events $F^z \subseteq F$ and each starting event $i \in F^z$ has a time window $[l_i, u_i]$. If a vehicle k wants to use this charging event, it should start its charging at time $T_i^k \in [l_i, u_i]$. This implies that charging events at a charging station have strict time windows and electric buses cannot start charging outside these time windows. Although this formulation can cover the general case where one allocates specific time windows for the start of charging at a charger, some chargers might be available without any time window restrictions. In that case, a charger is available as long as it is not occupied by a vehicle. This can be incorporated in our mathematical formulation by introducing *virtual* charging events.

We hereby explain the idea of *virtual* charging events. Consider a charging station $z \in Z$ that can be used by any vehicle as long as

it is not occupied by another vehicle and there are no time window restrictions on the starting times of charging. In that case, we can generate a number of virtual charging events F^z where each charging event $i \in F^z$ has the same time window $[l_i, u_i]$ corresponding to the start and end time of the planning horizon. This would imply that any vehicle k can charge at charger z at any time during the planning horizon because there would be an available charging event $i \in F^z$ such that $l_i \leq T_i^k \leq u_i$. The only requirement imposed to that vehicle with respect to using this charger is that the charger should not be occupied by another vehicle, which is enforced by constraints (25) and (26). Finally, we note that the virtual charging events $F^z = \{1, 2, \ldots, |F^z|\}$ should be enough so that the charger can be used repeatedly, if needed. This can be ensured by using a high number of charging events and the solution of the mathematical program will decide which ones of them will be used in practice. Because the virtual charging events have the same time window, we can arbitrary order them in the set $F^z = \{1, 2, \ldots, |F^z|\}$ without affecting the results of the optimization problem. Indeed, it is irrelevant which specific charging events of a charger will be used during the optimization because they all have the same start and end time. The only relevant part is the number of used charging events that will indicate how many times the charger was used during the planning period. This is made explicit later in our manuscript in our demonstration network 5.2.

3.4. EB-MDVSPTW Linearizations

Our EB-MDVSPTW formulation in Eqs. (27)-(29) is nonlinear and this does not guarantee that locally optimal solutions are globally optimal ones. Especially the nonlinearities in the problem's constraints result in a non-convex feasible region that has unwanted repercussions when trying to find a globally optimal solutions. Herein we propose the linearization of nonlinear constraints. We start with constraints (12),(13),(14) expressed as:

$$x_{ij}^k(T_i^k + \tilde{t}_i + t_{ij}) \leq x_{ij}^k T_j^k \qquad \forall k \in K\ \forall (i,j) \in A^k \mid i \in V^k$$
$$x_{o_k j}^k(T_{o_k}^k + t_{o_k j}) \leq x_{o_k j}^k T_j^k \qquad \forall k \in K\ \forall (o_k, j) \in A^k$$
$$x_{ij}^k(T_i^k + \tau_i^k + \tilde{t}_{ij}) \leq x_{ij}^k T_j^k \qquad \forall k \in K\ \forall (i,j) \in A^k \mid i \in F$$

Let us introduce continuous variables $\sigma_{ij}^k \in \mathbb{R}$ for $(i,j) \in A^k, k \in K$. Then, constraints (12),(13),(14) can be linearized by replacing them with constraints (30)-(34) according to the following proposition.

Proposition 3.1. *The linear inequality constraints:*

$$T_i^k + \tilde{t}_i + t_{ij} - T_j^k + \sigma_{ij}^k \leq 0 \qquad \forall k \in K\ \forall (i,j) \in A^k \mid i \in V^k \tag{30}$$

$$T_{o_k}^k + t_{o_k j} - T_j^k + \sigma_{o_k j}^k \leq 0 \qquad \forall k \in K\ \forall (o_k, j) \in A^k \tag{31}$$

$$T_i^k + \tau_i^k + t_{ij} - T_j^k + \sigma_{ij}^k \leq 0 \qquad \forall k \in K\ \forall (i,j) \in A^k \mid i \in F \tag{32}$$

$$\sigma_{ij}^k \leq M(1 - x_{ij}^k) \qquad \forall k \in K\ \forall (i,j) \in A^k \tag{33}$$

$$\sigma_{ij}^k \geq -M(1 - x_{ij}^k) \qquad \forall k \in K\ \forall (i,j) \in A^k \tag{34}$$

are equisatisfiable with the nonlinear constraints:

$$x_{ij}^k(T_i^k + \tilde{t}_i + t_{ij}) \leq x_{ij}^k T_j^k \qquad \forall k \in K\ \forall (i,j) \in A^k \mid i \in V^k \tag{12}$$

$$x_{o_k j}^k(T_{o_k}^k + t_{o_k j}) \leq x_{o_k j}^k T_j^k \qquad \forall k \in K\ \forall (o_k, j) \in A^k \tag{13}$$

$$x_{ij}^k(T_i^k + \tau_i^k + \tilde{t}_{ij}) \leq x_{ij}^k T_j^k \qquad \forall k \in K\ \forall (i,j) \in A^k \mid i \in F \tag{14}$$

Proof. For $x_{ij}^k = 1$ for some $(i,j) \in A^k \mid i \in V^k$ constraints (12) will require that $T_j^k \geq T_i^k + \tilde{t}_i + t_{ij}$. Similarly, for $x_{ij}^k = 1$ for some $(i,j) \in A^k \mid i \in V^k$ constraints (33) and (34) will impose that $\sigma_{ij}^k = 0$ and constraints (30) will require that $T_j^k \geq T_i^k + \tilde{t}_i + t_{ij}$. Thus, constraints (30),(33)-(34) and constraints (12) are equisatisfiable. For $x_{ij}^k = 0$ for some $(i,j) \in A^k \mid i \in V^k$ constraints (12) are satisfied for any T_i^k, T_j^k. Similarly, for $x_{ij}^k = 0$ for some $(i,j) \in A^k \mid i \in V^k$ constraints (33) and (34) will allow σ_{ij}^k to take any real value in the range $[-M, M]$, where M is a very large positive number. Thus, constraints (30) can be satisfied for any T_i^k, T_j^k since $\exists\ \sigma_{ij}^k \in [-M, M]$ such that $T_i^k + t_{ij} + \tilde{t}_i - T_j^k + \sigma_{ij}^k \leq 0$ for $M \to +\infty$. By the same token, constraints (13) and constraints (31),(33)-(34) are equisatisfiable. The same holds true for constraints (14) and constraints (32),(33)-(34). □

In addition, the nonlinear constraints:

$$e_j^k \geq (\bar{e}_i^k - \theta_{ij}) x_{ij}^k \qquad \forall (i,j) \in A^k,\ \forall k \in K \tag{20}$$

can be replaced by the following equisatisfiable set of linear inequality constraints, where $\bar{\sigma}_{ij}^k$ are newly introduced continuous variables:

$$e_j^k \geq (\bar{e}_i^k - \theta_{ij}) + \bar{\sigma}_{ij}^k \qquad \forall (i,j) \in A^k,\ \forall k \in K \tag{35}$$

$$\bar{\sigma}_{ij}^k \leq M(1 - x_{ij}^k) \qquad \forall (i,j) \in A^k,\ \forall k \in K \tag{36}$$

$$\bar{\sigma}_{ij}^k \geq -M(1 - x_{ij}^k) \qquad \forall (i,j) \in A^k,\ \forall k \in K \tag{37}$$

Finally, nonlinear constraints (26):

$$\sum_{k \in K} y_i^k \left(T_i^k + \tau_i^k\right) \leq T_{\omega_i}^k + M\left(1 - \sum_{\rho:(\omega_i,\rho) \in A^k} x_{\omega_i \rho}^k\right) \quad \forall i \in F_0,\ \forall k \in K$$

can be linearized according to the following proposition by adding continuous variables $\tilde{\sigma}_i^{k_0}$ for all $i \in F$ and $k_0 \in K$:

Proposition 3.2. *The linear inequality constraints:*

$$T_i^{k_0} + \tau_i^{k_0} + \tilde{\sigma}_i^{k_0} \leq T_{\omega_i}^k + M\left(1 - \sum_{\rho:(\omega_i,\rho) \in A^k} x_{\omega_i \rho}^k\right)$$
$$\forall i \in F_0\ \forall k \in K\ \forall k_0 \in K \tag{38}$$

$$\tilde{\sigma}_i^{k_0} \leq M(1 - y_i^{k_0}) \qquad \forall i \in F_0\ \forall k_0 \in K \tag{39}$$

$$\tilde{\sigma}_i^{k_0} \geq -M(1 - y_i^{k_0}) \qquad \forall i \in F_0\ \forall k_0 \in K \tag{40}$$

are equisatisfiable with the nonlinear constraints:

$$\sum_{k \in K} y_i^k (T_i^k + \tau_i^k) \leq T_{\omega_i}^k + M\left(1 - \sum_{\rho:(\omega_i,\rho) \in A^k} x_{\omega_i \rho}^k\right) \quad \forall i \in F_0,\ \forall k \in K \tag{26}$$

Proof. Consider the left-hand side of constraints (26). Because of constraints (9) at most one vehicle will perform charging event $i \in F$. That is, $\sum_{k \in K} y_i^k \leq 1\ \ \forall i \in F_0$. Because y_i^k is a binary variable, this means that if there is some $k^* \in K$ for which $y_i^{k^*} = 1$, then $y_i^k = 0\ \ \forall k \in K \mid k \neq k^*$. Because of this we can rewrite (26) as:

$$y_i^{k_0}(T_i^{k_0} + \tau_i^{k_0}) \leq T_{\omega_i}^k + M\left(1 - \sum_{\rho:(\omega_i,\rho) \in A^k} x_{\omega_i \rho}^k\right)$$

$$\forall i \in F_0,\ \forall k \in K,\ \forall k_0 \in K$$

because these constraints are equisatisfiable. In more detail, if vehicle k_0 is not assigned to event $i \in F$ then the left-hand side $y_i^{k_0}(T_i^{k_0} + \tau_i^{k_0})$ is equal to 0 ensuring that the constraint is satisfied. If, however, k_0 is the vehicle for which $y_i^{k_0} = 1$ then the constraint becomes:

$$(T_i^{k_0} + \tau_i^{k_0}) \leq T_{\omega_i}^k + M\left(1 - \sum_{\rho:(\omega_i,\rho)\in A^k} x_{\omega_i\rho}^k\right) \quad \forall i \in F_0,\ \forall k \in K$$

Equivalently, if $y_i^{k_0} = 1$ for some $k_0 \in K$ then $\sum_{k\in K} y_i^k(T_i^k + \tau_i^k) = (T_i^{k_0} + \tau_i^{k_0})$ because $y_i^k = 0$ for any other $k \in K$. This proves that we can write constraints (26) as:

$$y_i^{k_0}(T_i^{k_0} + \tau_i^{k_0}) \leq T_{\omega_i}^k + M\left(1 - \sum_{\rho:(\omega_i,\rho)\in A^k} x_{\omega_i\rho}^k\right)$$
$$\forall i \in F,\ \forall k \in K,\ \forall k_0 \in K$$

Now, we can replace $y_i^{k_0}(T_i^{k_0} + \tau_i^{k_0})$ by $(T_i^{k_0} + \tau_i^{k_0}) + \tilde{\sigma}_i^{k_0}$ where $\tilde{\sigma}_i^{k_0} \in \mathbb{R}$ is forced to take the value of 0 for $y_i^{k_0} = 1$ because of constraints (39)-(40), and any other value such that Eq. (38) is satisfied for $y_i^{k_0} = 0$ because in that case $\tilde{\sigma}_i^{k_0} \in [-M, M]$. □

Having linearized all nonlinear constraints, we now turn our attention to the nonlinear objective function:

$$\min \sum_{k\in K} \sum_{(i,j)\in A_k \mid i\in V^k} \left(b_{ij}^k + \lambda(T_j^k - T_i^k - \tilde{t}_i - t_{ij})\right)x_{ij}^k + \sum_{k\in K} \sum_{(i,j)\in A_k \mid i\in F} \left(b_{ij}^k + \lambda(T_j^k - T_i^k - \tau_i^k - t_{ij})\right)x_{ij}^k$$

We introduce continuous variables z_{ij}^k that should take the value of $(b_{ij}^k + \lambda(T_j^k - T_i^k - \tilde{t}_i - t_{ij}))x_{ij}^k$ for $(i,j) \in A_k \mid i \in V^k$ and $(b_{ij}^k + \lambda(T_j^k - T_i^k - \tau_i^k - t_{ij}))x_{ij}^k$ for $(i,j) \in A_k \mid i \in F$. This is enforced by the following set of linear inequality constraints:

$$z_{ij}^k \leq x_{ij}^k M \qquad \forall k \in K, (i,j) \in A_k \mid i \in V^k \cup F \tag{41}$$

$$z_{ij}^k \geq -x_{ij}^k M \qquad \forall k \in K, (i,j) \in A_k \mid i \in V^k \cup F \tag{42}$$

$$z_{ij}^k \leq b_{ij}^k + \lambda\left(T_j^k - T_i^k - \tilde{t}_i - t_{ij}\right) + M\left(1 - x_{i,j}^k\right)$$
$$\forall k \in K, (i,j) \in A_k \mid i \in V^k \tag{43}$$

$$z_{ij}^k \leq b_{ij}^k + \lambda\left(T_j^k - T_i^k - \tau_i^k - t_{ij}\right) + M\left(1 - x_{i,j}^k\right)$$
$$\forall k \in K, (i,j) \in A_k \mid i \in F \tag{44}$$

$$z_{ij}^k \geq b_{ij}^k + \lambda\left(T_j^k - T_i^k - \tilde{t}_i - t_{ij}\right) - \left(1 - x_{ij}^k\right)M$$
$$\forall k \in K, (i,j) \in A_k \mid i \in V^k \tag{45}$$

$$z_{ij}^k \geq b_{ij}^k + \lambda\left(T_j^k - T_i^k - \tau_i^k - t_{ij}\right) - \left(1 - x_{ij}^k\right)M$$
$$\forall k \in K, (i,j) \in A_k \mid i \in F \tag{46}$$

The objective function is then replaced by:

$$\min \sum_{k\in K} \sum_{(i,j)\in A_k \mid i\in V^k\cup F} z_{ij}^k$$

It remains to prove that $z_{ij}^k = (b_{ij}^k + \lambda(T_j^k - T_i^k - \tilde{t}_i - t_{ij}))x_{ij}^k$ for $(i,j) \in A_k \mid i \in V^k$ and $z_{ij}^k = (b_{ij}^k + \lambda(T_j^k - T_i^k - \tau_i^k - t_{ij}))x_{ij}^k$ for $(i,j) \in A_k \mid i \in F$. Let us first focus on the case:

$$z_{ij}^k = \left(b_{ij}^k + \lambda(T_j^k - T_i^k - \tilde{t}_i - t_{ij})\right)x_{ij}^k \qquad \forall k \in K,\ (i,j) \in A_k \mid i \in V^k$$

Notice that if $x_{ij}^k = 0$ we have that $(b_{ij}^k + \lambda(T_j^k - T_i^k - \tilde{t}_i - t_{ij}))x_{ij}^k$ and thus z_{ij}^k should be equal to 0. This is enforced by inequality constraints (41) and (42). If $x_{ij}^k = 1$ we have that z_{ij}^k should be equal to $b_{ij}^k + \lambda(T_j^k - T_i^k - \tilde{t}_i - t_{ij})$. This is enforced by inequality constraints (43) and (45) which require that:

$$b_{ij}^k + \lambda(T_j^k - T_i^k - \tilde{t}_i - t_{ij}) \leq z_{ij}^k \leq b_{ij}^k + \lambda\left(T_j^k - T_i^k - \tilde{t}_i - t_{ij}\right)$$
$$\forall k \in K,\ (i,j) \in A_k \mid i \in V^k$$

forcing z_{ij}^k to be exactly equal to $b_{ij}^k + \lambda(T_j^k - T_i^k - \tilde{t}_i - t_{ij})$.

Similarly, inequality constraints (44) and (46) enforce z_{ij}^k to be exactly equal to $b_{ij}^k + \lambda(T_j^k - T_i^k - \tau_i^k - t_{ij})$ for all $k \in K,\ (i,j) \in A_k \mid i \in F$.

Using the linearizations of nonlinear constraints (12),(13),(14),(20) and (26) results in the following mixed-integer program with linear objective function and linear (in)equality constraints.

Linearized EB-MDVSPTW:

$$\min \sum_{k\in K} \sum_{(i,j)\in A_k \mid i\in V^k\cup F} z_{ij}^k \tag{47}$$

s.t.: vehicle scheduling constraints (8)-(11),(15)-(17),(30)-(34) (48)

electric charging constraints (18)-(19),(21)-(25),(35)-(46) (49)

We note that the continuous relaxation of our linearized EB-MDVSPTW can be solved to global optimality. In more detail, the constraints of the linearized EB-MDVSPTW are affine/linear equality and inequality constraints. Considering its continuous relaxation where we drop all integralities, the feasible region consists of halfspaces and hyperplanes forming a polyhedron. As a polyhedron, the feasible region is a *convex set*. The objective function is linear, thus it is both *convex* and *concave*. Because our minimization problem has a convex objective function and a convex feasible region, any locally optimal solution is a globally optimal one. In addition, EB-MDVSPTW is NP-Hard, as presented in the following theorem.

Theorem 3.3. *EB-MDVSPTW is NP-Hard.*

Proof. We can cast EB-MDVSPTW as a decision problem with a 'yes' or 'no' answer by asking whether there exists feasible solution such that the objective function score:

$$\sum_{k\in K} \sum_{(i,j)\in A_k \mid i\in V^k\cup F} z_{ij}^k$$

is less than or equal to a value ψ for a specific problem instance. Obviously, this decision problem is in NP because if an *oracle* provides a *certificate* z_{ij}^k, which is a solution to the problem, a deterministic Turing machine can check in polynomial time whether this solution is a 'yes' answer to the decision problem by checking whether

$$\sum_{k\in K} \sum_{(i,j)\in A_k \mid i\in V^k\cup F} z_{ij}^k \leq \psi$$

and whether the vehicle and charging constraints are satisfied. Note that the vehicle and electric charging constraints increase polynomially with the size of the problem and this is why all conditions in (48)-(49) can be checked in polynomial time.

We will further prove that the EB-MDVSPTW decision problem is NP-complete. We note that the EB-MDVSPTW decision problem seeks to find the *exact cover* $S^* = \{S_1, S_2, \ldots, S_k, \ldots\}$ of set V, where an *exact cover* of the trip set V is the set of feasible bus schedules $S_1, S_2, \ldots, S_k, \ldots$ that contain each trip $i \in V$ in exactly one of the bus schedules and satisfy the electric charging constraints. For instance, if S_k is the set of trips assigned to vehicle k, EB-MDVSPTW seeks to find the feasible exact cover $S^* = \{S_1, S_2, \ldots, S_k, \ldots\}$ such that $S_k \cap S_j = \emptyset$ for any pair of sets $S_k, S_j \in S^*$ and $\bigcup_{i=1,2,\ldots,k,\ldots} S_i = V$. The exact cover is one of Karp's 21 NP-complete decision problems. It is also poly-time reducible to the EB-MDVSPTW since we can use a polynomial time algorithm that translates problem instances of the exact cover decision problem to problem instances of the EB-MDVSPTW in such a way that the instance of one decision problem has a 'yes' answer if, and only if, the translated instance of the other decision problem has also a yes answer. Thus, EB-MDVSPTW is also NP-complete. Finally, the EB-MDVSPTW optimization problem presented in Eqs. (47)-(49) is NP-Hard because its decision problem is NP-complete. □

It is important to note that because EB-MDVSPTW is NP-Hard it cannot be solved for large problem instances. Approximate solutions can be derived for large problem instances with the use of (meta)heuristics, but there will be no guarantees that these approximate solutions are close to the globally optimal ones. Because of the computational intractability of EB-MDVSPTW, in the next section we provide valid inequalities that can tighet the solution space with the use of additional linear constraints aiming at reducing the computation times.

4. Valid inequalities

In this section we present valid inequalities that tighten the solution space, thus reducing the computational costs by accelerating the convergence to the optimal solution.

4.1. Arc set reductions

We can take advantage of the inter-node travel times and the lower/upper time bounds of starting every task at each node to reduce the set of feasible arcs for every vehicle $k \in K$. In more detail, set A_3^k can be reduced to:

$$A_3^k = (i, j) \quad \forall i \in V^k \quad \forall j \in V^k - \{i\} \text{ such that } l_i + \tilde{t}_i + t_{ij} \leq u_j$$

by removing all arcs (i, j) for which the lowest possible starting time at task i, (l_i), plus the travel time needed to complete task i and travel to the start of node j, $(\tilde{t}_i + t_{ij})$, is greater than the latest possible starting time of task j, (u_j). The same holds for the arcs in set A_4^k which are reduced to:

$$A_4^k = (i, j) \quad \forall i \in V^k \quad \forall j \in F \text{ such that } l_i + \tilde{t}_i + t_{ij} \leq u_j$$

In addition, the task performed at a charging event node $i \in F$ is a charging task that cannot last less than 0 seconds. That is,

$$A_5^k = (i, j) \quad \forall i \in F \quad \forall j \in V^k \text{ such that } l_i + t_{ij} \leq u_j$$

Because the task at the starting depot o_k lasts also 0 seconds, we also have:

$$A_1^k = (o_k, j) \quad \forall j \in N^k - \{o_k\} \text{ such that } l_{o_k} + t_{o_k j} \leq u_j$$

This results in the reduced arc set:

$$A^k = \begin{cases} A_1^k = (o_k, j) \quad \forall j \in N^k - \{o_k\} \text{ such that } l_{o_k} + t_{o_k j} \leq u_j \\ A_2^k = (j, d_k) \quad \forall j \in N^k - \{o_k, d_k\} \\ A_3^k = (i, j) \quad \forall i \in V^k \quad \forall j \in V^k - \{i\} \text{ such that } l_i + \tilde{t}_i + t_{ij} \leq u_j \\ A_4^k = (i, j) \quad \forall i \in V^k \quad \forall j \in F \text{ such that } l_i + \tilde{t}_i + t_{ij} \leq u_j \\ A_5^k = (i, j) \quad \forall i \in F \quad \forall j \in V^k \text{ such that } l_i + t_{ij} \leq u_j \end{cases}$$

4.2. SOC Reductions

We hereby propose further inequality constraints that exclude infeasible solutions from the solution space. First, the SOC of each vehicle $k \in K$ upon arrival at a node should be less than or equal the maximum SOC, $\phi_{\max}^k$:

$$e_j^k \leq \phi_{max}^k \quad \forall k \in K, \ \forall j \in V^k \cup F \cup \{d_k\} \tag{50}$$

In addition, a vehicle k should have enough leftover SOC after operating an arc $(i, j) \in A_k$ to operate it. If q_j is the closest charging node from j, this means that the SOC of vehicle k upon departure from j should be such that it allows it to travel to q_j. If this is not the case, traversing arc (i, j) is an infeasible option because after performing such action the leftover SOC of the vehicle will not suffice to travel to the closest charging node. This is expressed by the following inequality constraints that limit further the solution space:

$$\tilde{e}_j^k \geq \phi_{min}^k + \theta_{j,q_j} \quad \forall j \in K, \ \forall j \in V^k \tag{51}$$

In more detail, $\tilde{e}_j^k \geq \phi_{\min}^k + \theta_{j,q_j}$ ensures that even after consuming the required energy to execute task j the SOC of vehicle k, $\tilde{e}_j^k$, suffices to allow the vehicle to travel to the closest charging station q_j.

4.3. Charging event reductions

Notice that the left-hand side of the inequality constraints:

$$\sum_{k \in K} y_i^k (T_i^k + \tau_i^k) \leq T_{\omega_i}^k + M\left(1 - \sum_{\rho:(\omega_i,\rho)\in A^k} x_{\omega_i \rho}^k\right) \quad \forall i \in F_0, \ \forall k \in K \tag{26}$$

has the lower bound of:

$$\sum_{k \in K} y_i^k l_i$$

since $\sum_{k \in K} y_i^k (T_i^k + \tau_i^k) \geq \sum_{k \in K} y_i^k l_i$ for any $i \in F_0$.

Using this lower bound which expresses the earliest possible departure time from the charger of a vehicle that uses charging event i, we can add the following linear inequality constrains tightening further the solution space:

$$\sum_{k \in K} y_i^k l_i \leq T_{\omega_i}^k + M\left(1 - \sum_{\rho:(\omega_i,\rho)\in A^k} x_{\omega_i \rho}^k\right) \quad \forall i \in F_0, \ \forall k \in K \tag{52}$$

4.4. Service start time reductions

We further introduce constraints with respect to the feasibility of start times at task nodes. In particular, if the start time of a task of node i is T_i^k then vehicle k cannot travel to task node j if it arrives there late, e.g., after its upper bound time u_j. This is expressed in the following two valid inequalities that reduce further the solution space:

$$T_i^k + \tilde{t}_i + t_{ij} \leq u_j + M\left(1 - x_{ij}^k\right) \quad \forall i \in V^k, j \in V^k \cup F \cup \{d_k\} - \{i\} \tag{53}$$

$$T_i^k + \tau_i + t_{ij} \leq u_j + M\left(1 - x_{ij}^k\right) \qquad \forall i \in F, j \in V^k \cup \{d_k\} \qquad (54)$$

Note that the term $M(1 - x_{ij}^k)$ in the above valid inequalities ensures that the constrains are applied to arcs i, j which are used by vehicle k since we do not need to impose constraints to unused arcs.

4.5. Conflicting arc reductions

Finally, we note that adjacent arcs in our graph $G = \{N, A\}$ might be *in conflict*, meaning that they cannot be part of the solution simultaneously. For this, we expand the definition of in-conflict arcs provided in Hadjar, Marcotte, & Soumis (2006) by considering also the incoming/outgoing arcs to/from charging events.

Definition 4.1. Let i, j, k and i', j', k' be two adjacent arcs of multigraph G. We say that they are *in conflict* if $k = k'$ or $i = i'$ or $j = j'$. That is, they are in conflict if they cannot appear in the a feasible solution of the EB-MDVSPTW instance.

Because they cannot appear in a feasible solution of the EB-MDVSPTW, we remove these arcs by using the following valid inequalities:

$$x_{ij}^k + x_{ij}^{k'} \leq 1 \qquad \forall k \in K, \forall k' \in K - \{k'\}, \forall (i,j) \in A_k \cap A_k' \qquad (55)$$

$$x_{ij}^k + x_{i'j'}^k \leq 1 \quad \forall k \in K, \forall (i,j) \in A_k, \forall (i',j') \in A_k : i' = i \wedge j' \neq j \qquad (56)$$

$$x_{ij}^k + x_{i'j'}^k \leq 1 \quad \forall k \in K, \forall (i,j) \in A_k, \forall (i',j') \in A_k : i' \neq i \wedge j' = j \qquad (57)$$

Adding these valid inequalities to the linearized EB-MDVSPTW result in the following problem:

Linearized EB-MDVSPTW with Valid Inequalities:

$$\min \sum_{k \in K} \sum_{(i,j) \in A_k \mid i \in V^k \cup F} z_{ij}^k \qquad (58)$$

s.t.: vehicle scheduling constraints (8)-(11),(15)-(17),(30)-(34) (59)

electric charging constraints (18)-(19),(21)-(25),(35)-(46) (60)

valid inequalities (50)-(57) (61)

The resulting problem is a mixed-integer linear program. Analyzing its time complexity, because of the integer nature of the problem it can be solved with simple enumeration or more effective methods, such as branch-and-cut. Branch-and-cut explores the solution space more efficiently by forming a rooted tree that contains all candidate solutions and using cutting planes to tighten the linear programming relaxations. We can then exclude parts of this tree based on the performance of its nodes. To evaluate the performance of each node of the tree we need to solve a relaxed continuous linear program. Even if continuous linear programs can be solved in polynomial time using Karmarkar's interior point algorithm (Karmarkar, 1984) with time complexity of $O(n^{3.5}L^2)$ where n is the total number of variables and L the number of bits of input to the algorithm, the nodes of the rooted tree might require to explore all solution candidates at the worst-case scenario. Thus, the computational complexity of the problem is exponential.

Table 3
Time window of each task node.

Task node	l_i	u_i	Task node	l_i	u_i
o_1	0	20	1001	20	270
o_2	0	20	1011	220	470
d_1	800	6000	1002	420	670
d_2	800	6000	1012	640	870
1	20	240	1003	40	1090
2	420	640	1013	1040	3790
3	40	260	1004	440	1990
4	440	1060	1014	1240	3890
5	820	2820			
6	840	4840			

5. Demonstration in a toy network

We hereby provide a demonstration of the application of our model in a toy network. The toy network is small in order to describe the input and the output of our model in detail, enhancing its reproducibility. In this network we consider two electric bus lines with 3 trips each. The trips of the first line are trips 1, 2, and 5 and the trips of the second line are trips 3, 4, and 6. These trips should be performed by two vehicles $K = \{1, 2\}$. The first vehicle should start from depot o_1 with coordinates (677908, 6150220) representing the latitude and longitude in the geographic coordinate system, respectively. It should also return to depot d_1 with coordinates (585053, 6140355). The second vehicle should start from depot o_2 with coordinates (677908, 6150220) and finish its trip at depot d_2 with coordinates (720134, 6210199). Note that depots o_1 and o_2 are at the same physical location, whereas depots d_1 and d_2 are at different locations. In addition to that, we have four charging stations $Z = \{1, 2, 3, 4\}$ and a set of 8 charging events $F = \{1001, 1011, 1002, 1012, 1003, 1013, 1004, 1014\}$. Charging events 1001 and 1011 can be performed in charger 1, charging events 1002 and 1012 in charger 2, and so forth.

The complete set of task nodes N is:

$$N = \{o_1, o_2, 1, 2, 3, 4, 5, 6, d_1, d_2, 1001, 1011, 1002, 1012, 1003, 1013, 1004, 1014\}$$

and the set of trips $V = \{1, 2, 3, 4, 5, 6\}$. Each vehicle is theoretically allowed to perform any trip, thus $V^1 = V^2 = \{1, 2, 3, 4, 5, 6\}$ and

$$N^1 = \{o_1, 1, 2, 3, 4, 5, 6, d_1, 1001, 1011, 1002, 1012, 1003, 1013, 1004, 1014\}$$

, whereas

$$N^2 = \{o_2, 1, 2, 3, 4, 5, 6, d_2, 1001, 1011, 1002, 1012, 1003, 1013, 1004, 1014\}$$

The coordinates of all task nodes N are presented in the appendix Table A.12. Note that the trip nodes $V = \{1, 2, 3, 4, 5, 6\}$ have different coordinates (latitude and longitude) for their origin and destination locations symbolizing the first and the last stop of the trip, whereas the depot nodes o_1, o_2, d_1, d_2 and the charging event nodes F have the same origin and destination coordinates because when performing such tasks the vehicle remains idle (i.e., the vehicle does not change its physical location while charging or while waiting at a depot).

Based on the Euclidean distance between the coordinates of nodes, we compute the travel time $\tilde{t}_i$ and consumed energy η_i when performing trip $i \in V$. These values are presented in the appendix Table A.13. The travel times from the end node of one event $i \in N$ to the start node of another event $j \in N$ are presented in the appendix Table A.14. Similarly, the energy consumption θ_{ij} from the end node of one event $i \in N$ to the start node of another event $j \in N$ is presented in the appendix Table A.15.

Table 4
Time T_i^k that service begins at each visiting node i by vehicle $k = 1$.

	visiting nodes								
	o_1	1	1003	4	1004	5	1013	6	d_1
l_i	0	20	40	820	440	840	1040	800	800
T_i^k	0	153.58	570.65	734.85	1127.61	1234.72	1651.79	1789.39	2100.96
u_i	20	240	1090	2820	1990	4840	3790	6000	6000
e_i^k	n/a	746.60	58.43	915.50	267.49	968.32	280.14	915.50	401.41
$\tilde{e}_i^k$	1000	411.40	1000	614.15	1000	633.12	1000	614.15	n/a
τ_i^k	n/a	n/a	112.99	n/a	87.91	n/a	86.38	n/a	n/a

Table 5
Time T_i^k that service begins at each visiting node i by vehicle $k = 2$.

	visiting nodes				
	o_1	3	1002	2	d_1
l_i	0	440	420	420	800
T_i^k	7.20	156.22	475.77	640.00	877.09
u_i	20	1060	670	640	6000
e_i^k	n/a	754.13	226.86	882.10	490.91
$\tilde{e}_i^k$	1000	452.78	1000	546.91	n/a
τ_i^k	n/a	n/a	92.78	n/a	n/a

5.1. Solution in case of charging events with time windows

The time window of each task node is also provided in Table 3. Note that the charging events have also a time window.

We also consider $\lambda = 1$ as the unit waiting cost of a vehicle, $\phi_{\max}^k = 1000$, $\phi_{\min}^k = 10$, and $r = 50/6$ expressed in consumed energy per minute.

Our MILP is programmed in Python 3.7 and solved by Gurobi using branch-and-cut and dual simplex. The globally optimal solution has a cost of 1433.44 resulting in:

- vehicle 1 serving the task node sequence $o_1 \rightarrow 1 \rightarrow 1003 \rightarrow 4 \rightarrow 1004 \rightarrow 5 \rightarrow 1013 \rightarrow 6 \rightarrow d_1$
- vehicle 2 serving the task node sequence $o_2 \rightarrow 3 \rightarrow 1002 \rightarrow 2 \rightarrow d_2$.

The time that service begins at each visiting node i by vehicle $k \in K$, T_i^k, is presented in Table 4 for vehicle 1 and Table 5 for vehicle 2. Note that these service times are within the imposed lower and upper bound values. In these tables we also present the SOC upon arrival, e_i^k, and upon departure, $\tilde{e}_i^k$, from each visiting task node together with the charging time τ_i^k. Note that all SOC values are within the range $[\phi_{\min}^k, \phi_{\max}^k] = [10, 1000]$. Of specific interest is the fact that vehicle $k = 1$ visits charger 3 twice, during charging events 1003 and 1013. Note that $(T_{1003}^1, \tau_{1003}^1) = (570.65, 122.99)$ and $T_{1013}^1 = 1651.79$ ensuring the satisfaction of constraint (38) that does not permit the simultaneous occupation of one charger by two vehicles because:

$$T_{1003}^1 + \tau_{1003}^1 \leq T_{1013}^1 \text{ since } 570.65 + 122.99 \leq 1651.79$$

5.2. Solution in case of charging events without time windows

Let us now consider the case that we can freely use any charger as long as it is not occupied by another vehicle. In that case, we generate a large number of virtual charging events for each one of the 4 chargers where each charging event $i \in F$ has a time window $[l_i, u_i] = [0, 6000]$ which corresponds to the start and end time of our planning period given that a vehicle can start from the depot after time 0 and return to it before time 6000. We introduce charging events $F^1 = \{1001, 1011, 1021, 1031\}$ that can be performed in charger 1, $F^2 = \{1002, 1012, 1022, 1032\}$ that can be performed in charger 2, and so on. All these charging events have a time window of [0,6000]. We then solve the optimization problem resulting in solution:

- vehicle 1 serving the task node sequence $o_1 \rightarrow 1 \rightarrow 1001 \rightarrow 4 \rightarrow 6 \rightarrow 1012 \rightarrow 5 \rightarrow d_1$
- vehicle 2 serving the task node sequence $o_2 \rightarrow 3 \rightarrow 1002 \rightarrow 2 \rightarrow d_2$.

with a reduced cost of 1279.69. This cost reduction is expected because now a vehicle can start charging at any charger at any time provided that the charger is not occupied by another vehicle. Note that we introduced four virtual charging events per charger and our optimal solution used only 2 charging events from charger 2 (1002 and 1012) and 1 from charger 1 (1001), whereas chargers 3 and 4 were not used at all.

6. Computational results

In this section we perform computational experiments in larger instances to explore the computational complexity of our approach. A set of EB-MDVSPTW benchmark instances are generated in a way similar to the generation of the MD-VSP instances in Carpaneto, Dell'Amico, Fischetti, & Toth (1989) used by other researchers (see Bianco, Mingozzi, & Ricciardelli (1994); Fischetti, Lodi, Martello, & Toth (2001); Forbes, Holt, & Watts (1994); Ribeiro & Soumis (1994). The depots and the starting and ending points of the trips are distributed in a 60 km by 60 km square in the Euclidean plane using a uniform distribution. The travel times between nodes, in minutes, are equal to the Euclidean distances between the nodes. That is, a vehicle drives 60km in 1 h. The problems are solved with no restriction on trip/depot combinations. The waiting time cost λ is 2 units per minute and the travel time cost is taken to be 10 units per minute, resulting in $b_{ij}^k = 10t_{ij}$ for all $k \in K$.

The upper bound of the time associated to each node $i \in N$ is equal to the lower bound plus a value in [200,300,400] depending on the instance size (10 trips, 20 trips, 30 trips). A set of recharging stations are also distributed in a 60 km by 60 km square in the Euclidean plane. The vehicle driving range, the charging rate and the remaining parameter values are made publicly available in our generated benchmark instances on Github (2021), which also includes the software code of the Linearized EB-MDVSPTW and the Linearized EB-MDVSPTW with Valid Inequalities. The software code of the models and the benchmark instances are made publicly available to facilitate the reproducibility of the numerical experiments.

Table 6 describes 4 classes of instances. For each class we list the number of trips, the number of depots, the number of stations as well as the number of instances generated. The generated instances with up to 30 trips are solved by Gurobi 9.1.2 using branch-and-cut and dual simplex. All experiments were conducted on a conventional computer machine with 16GB RAM and an Intel(R) Core(TM) i7-4790 CPU @ 3.60GHz processor. The termination cri-

Table 6
EB-MDVSPTW instances.

Name	Vehicles	Depots	Chargers	Charging Events	Trips	Instances
D2_S2_C10	2	2	2	8	10	5
D2_S4_C10	2	2	4	8	10	5
D2_S3_C20	3	2	2	4	20	5
D2_S3_C30	3	2	2	4	30	5

Table 7
Results for 10-trip instances. CNS: Constraints, NE: B&B Nodes Evaluated, SI: Simplex Iterations, CT: Computation Time in minutes, SP: Solution Performance, OG: Optimality Gap.

Instance	Without valid inequalities				With valid inequalities				SP	OG
	CNS	NE	SI	CT	CNS	NE	SI	CT		
D2_S2_C10_a	6652	47,649	1,436,073	6.03	23,766	27,553	1,378,825	3.82	1909.32	0%
D2_S2_C10_b	6652	22,618	629,266	1.92	23,766	20,548	1,228,824	1.86	1478.27	0%
D2_S2_C10_c	6652	807,882	18,456,066	20.92	23,766	47,087	1,941,301	4.33	2292.79	0%
D2_S2_C10_d	6652	305,872	8,531,108	7.08	23,766	24,188	1,243,038	3.23	1338.73	0%
D2_S2_C10_e	6652	29,980	1,072,180	3.49	23,766	21,149	1,311,466	2.71	1774.88	0%
D2_S4_C10_a	6644	83,304	2,241,019	3.95	23,872	27,592	1,156,232	3.65	2355.38	0%
D2_S4_C10_b	6644	54,142	1,782,874	2.55	23,872	24,401	1,400,807	3.33	1661.05	0%
D2_S4_C10_c	6644	321,673	9,639,872	8.12	23,872	23,849	1,250,483	4.40	2008.29	0%
D2_S4_C10_d	6644	41,052	1,194,305	1.72	23,872	21,328	1,236,936	2.64	1722.26	0%
D2_S4_C10_e	6644	253,718	6,113,678	5.64	23,872	21,619	1,403,175	4.1	2116.74	0%
Average		196,789	5,109,644	7.89		25,931	1,355,109	3.19		

teria of the solver were either the convergence to the globally optimal solution or reaching a computational time limit of 5 hours.

In the numerical experiments we solve our Linearized EB-MDVSPTW model without valid inequalities (Eqs. (47)-(49)) and our Linearized EB-MDVSPTW model with valid inequalities (Eqs. (58)-(61)) to demonstrate the changes in the compactness of the problem (i.e., increase of constraints) and the changes in tightness (i.e., reduction of explored nodes in the rooted B&B tree and simplex iterations until convergence) when considering valid inequalities. This allows us to examine the trade-off between the increase of the problem size and the reduction of the computational complexity when using valid inequalities. We conducted experiments with up to 30 trips because beyond that the Linearized EB-MDVSPTW model that does not consider valid inequalities is not able to converge to a globally optimal solution within the 5-hour limit.

The results for the 10-trip instances D2_S2_C10 and D2_S4_C10 are shown in Table 7. For each instance, the number of constraints (CNS), the number of nodes explored in the rooted tree (NE), the number of simplex iterations (SI), the computational time (CT) in minutes, the solution performance (SP) and the optimality gap (OG) are shown for both formulations.

As seen in Table 7, the computational performance of the model including valid inequalities is superior to that of the model without these. In 8 out of 10 instances computational times are shorter when using valid inequalities. We have up to 380% savings for a certain instance (D2_S2_C10_c), despite the three-fold increase in the number of constraints due to the addition of the valid inequalities. In general, due to the small size of these instances, they can be solved to optimality using either formulation – yet in more than double the computational time on average if valid inequalities are not considered.

We now proceed to the results of larger instances with 20 trips, as shown in Table 8 and Table 9.

As seen in Table 8, the addition of valid inequalities generally reduces the number of variables up to 20%, yet, at the same time, increases the number of constraints by almost 350%. The number of variables is reduced when including valid inequalities because the set of feasible arcs per vehicle, A^k, which controls the number of variables, is considerably smaller. In 4 out of 5 instances the number of nodes evaluated and the number of simplex iterations when using valid inequalities are approximately one third of the corresponding values when not using valid inequalities. In terms of computational times, there are notable savings in the former case compared to the latter, ranging from 33% to 73%.

Similar to the 10-trip case, all 20-trip instances are solved to optimality as well, as shown in Table 9. In this case, all but one instance can be solved with either formulation. In particular, instance D2_S3_C20_b was not solved to global optimality within the 5-hour computation time limit by the model that does not consider valid inequalities, resulting in a 2.49% optimality gap. In this specific instance, the gap between the best solution found by the solver (3139.22) and the lower bound value of the solver (2677.48) was 14.7%, meaning that the solver would have required significantly more time until the lower bound and the best-found solution values become the same, indicating convergence. In contrast, the same problem instance was solved to optimality in 282 minutes under the formulation with valid inequalities. Evidently, computational performance is largely dependent on input data, as indicated by the variability of solution times among the generated instances.

Finally, results for 30-trip instances are shown in Table 10 and Table 11.

As reported in Table 10, in this case as well, the addition of valid inequalities reduces the number of variables by 36% and increases the number of constraints by a factor of 4.5. In terms of tightness, the number of nodes explored and simplex iterations is significantly lower for the formulation under valid inequalities, with commensurate computational savings attained as well. In this case all instances are solved to optimality in 35 to 172 minutes, whereas in the case without inequalities the time limit is exhausted in all but one instances. The relative performance of the two formulations is shown in Table 11.

As shown in Table 11, the optimal solution was obtained in 3 out of 5 instances even without the addition of valid inequalities, with very small optimality gaps achieved in the remaining two cases. Still, convergence was notably slower for the formulation without valid inequalities, with non-zero lower bound gaps reported in 4 out of 5 cases. Apparently, under the current computational resources and modeling assumptions, instances over 30

Table 8
Results for 20-trip instances. VAR: Number of Variables, CNS: Constraints, NE: B&B Nodes Evaluated, SI: Simplex Iterations, CT: Computation Time.

Instance	Without valid inequalities					With valid inequalities				
	Compactness		Tightness			Compactness		Tightness		
	VAR	CNS	B&B NE	SI	CT	VAR	CNS	B&B NE	SI	CT
D2_S3_C20_a	7404	19,983	608,994	50,344,640	57.4	5844	72,048	164,877	21,441,235	31.6
D2_S3_C20_b	7404	19,983	2,072,153	202,967,196	300.0	6264	71,748	2,106,060	237,992,117	282.2
D2_S3_C20_c	7404	19,983	366,321	29,288,498	33.0	5832	71,850	96,849	10,267,253	20.4
D2_S3_C20_d	7404	19,983	1,868,906	162,017,226	172.7	5988	74,826	538,253	58,642,882	77.4
D2_S3_C20_e	7404	19,983	941,905	73,587,275	100.2	5808	71,370	146,975	18,479,778	26.8
Average	7404	19,983	1,171,656	103,640,967	132.7	5947	72,368	610,603	69,364,653	87.7

Table 9
Results for 20-trip instances. SP: Performance of best solution, LB: Lower Bound performance, LBG: Gap between the best solution and the Lower Bound, OG: Optimality Gap between the best solution and the globally optimal one.

Instance	Without valid inequalities				With valid inequalities	
	SP	LB	LBG	OG	SP	OG
D2_S3_C20_a	2868.44	2868.44	0%	0%	2868.44	0%
D2_S3_C20_b	3139.22	2677.48	14.70%	2.49%	3061.18	0%
D2_S3_C20_c	2656.39	2656.39	0%	0%	2656.39	0%
D2_S3_C20_d	2552.08	2552.08	0%	0%	2552.08	0%
D2_S3_C20_e	2864.46	2864.46	0%	0%	2864.46	0%

Table 10
Results for 30-trip instances. VAR: Number of Variables, CNS: Constraints, NE: B&B Nodes Evaluated, SI: Simplex Iterations, CT: Computation Time.

Instance	Without valid inequalities					With valid inequalities				
	Compactness		Tightness			Compactness		Tightness		
	VAR	CNS	B&B NE	SI	CT	VAR	CNS	B&B NE	SI	CT
D2_S3_C30_a	14,604	39,643	1,457,272	184,059,720	300	9300	139,642	463,924	53,355,756	85.8
D2_S3_C30_b	14,604	39,643	1,109,695	149,185,002	300	9324	140,206	814,656	75,911,714	172.4
D2_S3_C30_c	14,604	39,643	1,184,132	121,039,746	300	9312	139,918	623,155	66,360,830	113.0
D2_S3_C30_d	14,604	39,643	624,363	64,909,962	97.5	9336	140,434	291,187	51,326,133	77.3
D2_S3_C30_e	14,604	39,643	1,100,707	121,629,297	300	9336	140,500	103,973	13,272,067	35.6
Average	14,604	39,643	1,095,234	128,164,745	259.5	9322	140,140	459,379	52,045,300	96.8

Table 11
Results for 30-trip instances. SP: Performance of best solution, LB: Lower Bound performance, LBG: Gap between the best solution and the Lower Bound, OG: Optimality Gap between the best solution and the globally optimal one.

Instance	Without valid inequalities				With valid inequalities	
	SP	LB	LBG	OG	SP	OG
D2_S3_C30_a	5,917.15	5,680.01	4.00%	0%	5,917.15	0%
D2_S3_C30_b	5,929.31	5,356.40	9.67%	1.27%	5,854.07	0%
D2_S3_C30_c	4,203.48	3,739.05	11.00%	0%	4,203.48	0%
D2_S3_C30_d	4,969.23	4,969.23	0%	0%	4,969.23	0%
D2_S3_C30_e	5,901.43	5,461.83	7.45%	1.54%	5,810.73	0%

trips cannot be solved using the formulation without inequalities. As a general comment, it should be noted that the complexity of the problem grows with the width of time windows (Desrosiers, Dumas, Solomon, & Soumis, 1995), therefore computational savings can be attained by reducing these. Indeed, this is reflected in the relative performance of the model moving from 20-trip to 30-trip instances, as the reduction of time windows from 300 to 200 minutes, respectively, allows for only minimally increasing computational times, by just 10% for the case with valid inequalities.

Closing, it is important to note that being able to solve instances with 30 trips is in line with other exact methods for multi-depot vehicle scheduling problems for electric buses. For instance, Wen et al. (2016) were not able to solve instances with more than 30 trips with branch and cut (using CPLEX) even if that work used a simpler formulation without time windows on charging events and waiting costs due to the delayed start of tasks.

7. Conclusion

Vehicle scheduling for electric bus systems is a complex task, as limited energy and charging resources apply in this case. Moreover, the consideration of multi-use charging stations that do not exclusively serve buses, as well as charging windows for trips and charging events further complicate associated decisions. In this context, this study presents a mixed-integer non-linear formulation for the EB-MDVSPTW under time windows and charger scheduling constraints, considering opportunity charging at bus stops, terminal stations and mixed-use electric vehicle charging stations. The

proposed MINLP for the EB-MDVSPTW is then linearized and the resulting MILP can be solved to global optimality using an off-the-shelf solver. Furthermore, to tighten the solution space we introduce a set of valid inequalities, which we evaluate through computational experiments.

The proposed models (with and without valid inequalities) are first validated in a toy network and then applied to benchmark instances. Results on benchmark instances show the effectiveness of the proposed formulation with valid inequalities, yielding significant computational savings. The latter are in general more pronounced as the problem size grows. In fact, the formulation with the valid inequalities allows for solving instances with 30 trips to optimality, which could not be solved otherwise.

The proposed model can be extended in several ways. First, the model can be modified to consider partial recharging at designated charging stations, rather than allowing buses to fully charge their batteries. Second, additional considerations related to time-of-day electricity pricing may be incorporated, to more realistically assess energy-related costs. Third, uncertainty effects related to energy supply/consumption as well as traffic conditions may be taken into account through a robust optimization approach. Last, the model can be extended to also handle charger location concurrently with vehicle scheduling, addressing planning decisions pertaining to both strategic and tactical levels. In addition to the above, heuristic or metaheuristic approaches can be devised to reduce the computational cost of solving our MILP. In future research, one can devise such solution methods and study the trade-off between potential computation time improvements and optimality losses due to the use of heuristics/metaheuristics.

Appendix

Table A1
Event coordinates.

task node	origin location		destination location	
	latitude	**longitude**	**latitude**	**longitude**
o_1	677,908	6,150,220	677,908	6,150,220
o_2	677,908	6,150,220	677,908	6,150,220
1	538,181	6,086,484	720,415	6,176,264
2	538,181	6,086,484	720,415	6,176,264
3	528,913	6,152,557	710,831	6,168,718
4	528,913	6,152,557	710,831	6,168,718
5	538,181	6,086,484	720,415	6,176,264
6	528,913	6,152,557	710,831	6,168,718
d_1	585,053	6,140,355	585,053	6,140,355
d_2	720,134	6,210,199	720,134	6,210,199
1001	557,926	6,181,752	557,926	6,181,752
1011	557,926	6,181,752	557,926	6,181,752
1002	609,023	6,077,163	609,023	6,077,163
1012	609,023	6,077,163	609,023	6,077,163
1003	507,721	6,199,180	507,721	6,199,180
1013	507,721	6,199,180	507,721	6,199,180
1004	522,714	6,075,103	522,714	6,075,103
1014	522,714	6,075,103	522,714	6,075,103

Table A2
Travel time and consumed energy when performing each trip $i \in V$.

$i \in V$	$\tilde{t}_i$	η_i
1	203.1494	335.1965
2	203.1494	335.1965
3	182.6344	301.3468
4	182.6344	301.3468
5	203.1494	335.1965
6	182.6344	301.3468

Table A3
Travel times t_{ij} when deadheading from the end location of node $i \in N$ to the start location of node $j \in N$.

	o_1	o_2	1	2	3	4	5	6	d_1	d_2	1001/1011	1002/1012	1003/1013	1004/1014
o_1	0.00	0.00	153.58	153.58	149.01	149.01	153.58	149.01	93.38	73.35	124.06	100.41	177.09	172.42
o_2	0.00	0.00	153.58	153.58	149.01	149.01	153.58	149.01	93.38	73.35	124.06	100.41	177.09	172.42
1	49.85	49.85	0.00	203.15	192.96	192.96	203.15	192.96	140.04	33.94	162.58	149.09	213.92	222.08
2	49.85	49.85	203.15	0.00	192.96	192.96	203.15	192.96	140.04	33.94	162.58	149.09	213.92	222.08
3	37.76	37.76	191.23	191.23	0.00	182.63	191.23	182.63	128.94	42.51	153.46	136.92	205.38	210.12
4	37.76	37.76	191.23	191.23	182.63	0.00	191.23	182.63	128.94	42.51	153.46	136.92	205.38	210.12
5	49.85	49.85	203.15	203.15	192.96	192.96	0.00	192.96	140.04	33.94	162.58	149.09	213.92	222.08
6	37.76	37.76	191.23	191.23	182.63	182.63	191.23	0.00	128.94	42.51	153.46	136.92	205.38	210.12
d_1	93.38	93.38	71.41	71.41	57.45	57.45	71.41	57.45	0.00	152.07	49.49	67.59	97.16	90.24
d_2	73.35	73.35	220.03	220.03	199.72	199.72	220.03	199.72	152.07	0.00	164.68	173.33	212.70	239.22
1001/1011	124.06	124.06	97.29	97.29	41.16	41.16	97.29	41.16	49.49	164.68	0.00	116.40	53.14	112.31
1002/1012	100.41	100.41	71.45	71.45	110.01	110.01	71.45	110.01	67.59	173.33	116.40	0.00	158.59	86.33
1003/1013	177.09	177.09	116.74	116.74	51.21	51.21	116.74	51.21	97.16	212.70	53.14	158.59	0.00	124.98
1004/1014	172.42	172.42	19.20	19.20	77.70	77.70	19.20	77.70	90.24	239.22	112.31	86.33	124.98	0.00

Table A4
Consumed energy θ_{ij} when deadheading from the end location of node $i \in N$ to the start location of node $j \in N$.

	o_1	o_2	1	2	3	4	5	6	d_1	d_2	1001/1011	1002/1012	1003/1013	1004/1014
o_1	0.00	0.00	253.40	253.40	245.87	245.87	253.40	245.87	154.07	121.03	204.69	165.68	292.20	284.49
o_2	0.00	0.00	253.40	253.40	245.87	245.87	253.40	245.87	154.07	121.03	204.69	165.68	292.20	284.49
1	82.25	82.25	0.00	335.20	318.39	318.39	335.20	318.39	231.07	55.99	268.26	246.01	352.98	366.43
2	82.25	82.25	335.20	0.00	318.39	318.39	335.20	318.39	231.07	55.99	268.26	246.01	352.98	366.43
3	62.31	62.31	315.54	315.54	0.00	301.35	315.54	301.35	212.74	70.14	253.21	225.92	338.88	346.70
4	62.31	62.31	315.54	315.54	301.35	0.00	315.54	301.35	212.74	70.14	253.21	225.92	338.88	346.70
5	82.25	82.25	335.20	335.20	318.39	318.39	0.00	318.39	231.07	55.99	268.26	246.01	352.98	366.43
6	62.31	62.31	315.54	315.54	301.35	301.35	315.54	0.00	212.74	70.14	253.21	225.92	338.88	346.70
d_1	154.07	154.07	117.82	117.82	94.79	94.79	117.82	94.79	0.00	250.91	81.66	111.52	160.32	148.90
d_2	121.03	121.03	363.05	363.05	329.54	329.54	363.05	329.54	250.91	0.00	271.73	286.00	350.95	394.71
1001/1011	204.69	204.69	160.53	160.53	67.91	67.91	160.53	67.91	81.66	271.73	0.00	192.07	87.69	185.31
1002/1012	165.68	165.68	117.90	117.90	181.51	181.51	117.90	181.51	111.52	286.00	192.07	0.00	261.67	142.45
1003/1013	292.20	292.20	192.62	192.62	84.50	84.50	192.62	84.50	160.32	350.95	87.69	261.67	0.00	206.22
1004/1014	284.49	284.49	31.68	31.68	128.21	128.21	31.68	128.21	148.90	394.71	185.31	142.45	206.22	0.00

References

Abdelwahed, A., van den Berg, P. L., Brandt, T., Collins, J., & Ketter, W. (2020). Evaluating and optimizing opportunity fast-charging schedules in transit battery electric bus networks. *Transportation Science, 54*(6), 1601–1615.

Alvo, M., Angulo, G., & Klapp, M. A. (2021). An exact solution approach for an electric bus dispatch problem. *Transportation Research Part E: Logistics and Transportation Review, 156*, 102528.

Alwesabi, Y., Wang, Y., Avalos, R., & Liu, Z. (2020). Electric bus scheduling under single depot dynamic wireless charging infrastructure planning. *Energy, 213*, 118855.

An, K. (2020). Battery electric bus infrastructure planning under demand uncertainty. *Transportation Research Part C: Emerging Technologies, 111*, 572–587.

Bianco, L., Mingozzi, A., & Ricciardelli, S. (1994). A set partitioning approach to the multiple depot vehicle scheduling problem. *Optimization Methods and Software, 3*(1–3), 163–194.

Bie, Y., Ji, J., Wang, X., & Qu, X. (2021). Optimization of electric bus scheduling considering stochastic volatilities in trip travel time and energy consumption. *Computer-Aided Civil and Infrastructure Engineering*.

Bunte, S., & Kliewer, N. (2009). An overview on vehicle scheduling models. *Public Transport, 1*(4), 299–317.

Carpaneto, G., Dell'Amico, M., Fischetti, M., & Toth, P. (1989). A branch and bound algorithm for the multiple depot vehicle scheduling problem. *Networks, 19*(5), 531–548.

Chioni, E., Iliopoulou, C., Milioti, C., & Kepaptsoglou, K. (2020). Factors affecting bus bunching at the stop level: A geographically weighted regression approach. *International Journal of Transportation Science and Technology, 9*(3), 207–217.

Desaulniers, G., & Hickman, M. D. (2007). Public transit. *Handbooks in Operations Research and Management Science, 14*, 69–127.

Desaulniers, G., Lavigne, J., & Soumis, F. (1998). Multi-depot vehicle scheduling problems with time windows and waiting costs. *European Journal of Operational Research, 111*(3), 479–494.

Desrosiers, J., Dumas, Y., Solomon, M. M., & Soumis, F. (1995). Time constrained routing and scheduling. *Handbooks in Operations Research and Management Science, 8*, 35–139.

Esmailirad, S., Ghiasian, A., & Rabiee, A. (2021). An extended m/m/k/k queueing model to analyze the profit of a multiservice electric vehicle charging station. *IEEE Transactions on Vehicular Technology, 70*(4), 3007–3016.

Fischetti, M., Lodi, A., Martello, S., & Toth, P. (2001). A polyhedral approach to simplified crew scheduling and vehicle scheduling problems. *Management Science, 47*(6), 833–850.

Forbes, M., Holt, J., & Watts, A. (1994). An exact algorithm for multiple depot bus scheduling. *European Journal of Operational Research, 72*(1), 115–124.

Gao, Z., Lin, Z., LaClair, T. J., Liu, C., Li, J.-M., Birky, A. K., & Ward, J. (2017). Battery capacity and recharging needs for electric buses in city transit service. *Energy, 122*, 588–600.

Github (2021). EB-MDVSPTW models and benchmark instances. https://github.com/KGkiotsalitis/EB-MDVSPTW-, [Online; accessed 15-December-2021].

Gkiotsalitis, K. (2019). Bus rescheduling in rolling horizons for regularity-based services. *Journal of Intelligent Transportation Systems*, 1–20.

Gkiotsalitis, K. (2020). Bus holding of electric buses with scheduled charging times. *IEEE Transactions on Intelligent Transportation Systems*.

Gkiotsalitis, K. (2021). Improving service regularity for high-frequency bus services with rescheduling and bus holding. *Journal of Traffic and Transportation Engineering (English Edition)*.

Gkiotsalitis, K., & Alesiani, F. (2019). Robust timetable optimization for bus lines subject to resource and regulatory constraints. *Transportation Research Part E: Logistics and Transportation Review, 128*, 30–51.

Gkiotsalitis, K., & Cats, O. (2018). Reliable frequency determination: Incorporating information on service uncertainty when setting dispatching headways. *Transportation Research Part C: Emerging Technologies, 88*, 187–207.

Gkiotsalitis, K., & Cats, O. (2020). Timetable recovery after disturbances in metro operations: An exact and efficient solution. *IEEE Transactions on Intelligent Transportation Systems*.

Guschinsky, N., Kovalyov, M. Y., Rozin, B., & Brauner, N. (2021). Fleet and charging infrastructure decisions for fast-charging city electric bus service. *Computers & Operations Research, 135*, 105449.

Hadjar, A., Marcotte, O., & Soumis, F. (2006). A branch-and-cut algorithm for the multiple depot vehicle scheduling problem. *Operations Research, 54*(1), 130–149.

Haghani, A., & Banihashemi, M. (2002). Heuristic approaches for solving large-scale bus transit vehicle scheduling problem with route time constraints. *Transportation Research Part A: Policy and Practice, 36*(4), 309–333.

Häll, C. H., Ceder, A., Ekström, J., & Quttineh, N.-H. (2019). Adjustments of public transit operations planning process for the use of electric buses. *Journal of Intelligent Transportation Systems, 23*(3), 216–230.

He, Y., Liu, Z., & Song, Z. (2020). Optimal charging scheduling and management for a fast-charging battery electric bus system. *Transportation Research Part E: Logistics and Transportation Review, 142*, 102056.

Ibarra-Rojas, O. J., Delgado, F., Giesen, R., & Muñoz, J. C. (2015). Planning, operation, and control of bus transport systems: A literature review. *Transportation Research Part B: Methodological, 77*, 38–75.

Iliopoulou, C., & Kepaptsoglou, K. (2019a). Combining its and optimization in public transportation planning: State of the art and future research paths. *European Transport Research Review, 11*(1), 1–16.

Iliopoulou, C., & Kepaptsoglou, K. (2019b). Integrated transit route network design and infrastructure planning for on-line electric vehicles. *Transportation Research Part D: Transport and Environment, 77*, 178–197.

Iliopoulou, C., & Kepaptsoglou, K. (2021). Robust electric transit route network design problem (re-trndp) with delay considerations: Model and application. *Transportation Research Part C: Emerging Technologies, 129*, 103255.

Iliopoulou, C., Tassopoulos, I., Kepaptsoglou, K., & Beligiannis, G. (2019). Electric transit route network design problem: Model and application. *Transportation Research Record, 2673*(8), 264–274.

Iliopoulou, C. A., Milioti, C. P., Vlahogianni, E. I., & Kepaptsoglou, K. L. (2020). Identifying spatio-temporal patterns of bus bunching in urban networks. *Journal of Intelligent Transportation Systems, 24*(4), 365–382.

Jefferies, D., & Göhlich, D. (2020). A comprehensive tco evaluation method for electric bus systems based on discrete-event simulation including bus scheduling and charging infrastructure optimisation. *World Electric Vehicle Journal, 11*(3), 56.

Jovanovic, R., Bayram, I. S., Bayhan, S., & Voß, S. (2021). A grasp approach for solving large-scale electric bus scheduling problems. *Energies, 14*(20), 6610.

Karmarkar, N. (1984). A new polynomial-time algorithm for linear programming. In *Proceedings of the sixteenth annual acm symposium on theory of computing* (pp. 302–311).

Ke, B.-R., Chung, C.-Y., & Chen, Y.-C. (2016). Minimizing the costs of constructing an all plug-in electric bus transportation system: A case study in penghu. *Applied Energy, 177*, 649–660.

Kliewer, N., Amberg, B., & Amberg, B. (2012). Multiple depot vehicle and crew scheduling with time windows for scheduled trips. *Public Transport, 3*(3), 213–244.

Ko, Y. D., & Jang, Y. J. (2013). The optimal system design of the online electric vehicle utilizing wireless power transmission technology. *IEEE Transactions on Intelligent Transportation Systems, 14*(3), 1255–1265.

van Kooten Niekerk, M. E., Van den Akker, J., & Hoogeveen, J. (2017). Scheduling electric vehicles. *Public Transport, 9*(1), 155–176.

Kunith, A., Mendelevitch, R., & Goehlich, D. (2017). Electrification of a city bus network–an optimization model for cost-effective placing of charging infrastructure and battery sizing of fast-charging electric bus systems. *International Journal of Sustainable Transportation, 11*(10), 707–720.

Li, J.-Q. (2014). Transit bus scheduling with limited energy. *Transportation Science, 48*(4), 521–539.

Li, L., Lo, H. K., & Xiao, F. (2019). Mixed bus fleet scheduling under range and refueling constraints. *Transportation Research Part C: Emerging Technologies, 104*, 443–462.

Li, X., Wang, T., Li, L., Feng, F., Wang, W., & Cheng, C. (2020). Joint optimization of regular charging electric bus transit network schedule and stationary charger deployment considering partial charging policy and time-of-use electricity prices. *Journal of Advanced Transportation, 2020*.

Liu, K., Gao, H., Liang, Z., Zhao, M., & Li, C. (2021). Optimal charging strategy for large-scale electric buses considering resource constraints. *Transportation Research Part D: Transport and Environment, 99*, 103009.

Liu, T., & Ceder, A. A. (2020). Battery-electric transit vehicle scheduling with optimal number of stationary chargers. *Transportation Research Part C: Emerging Technologies, 114*, 118–139.

Liu, T., & Ceder, A. A. (2021). Research in public transport vehicle scheduling. In *Handbook of public transport research*. Edward Elgar Publishing.

Lu, T., Yao, E., Zhang, Y., & Yang, Y. (2021). Joint optimal scheduling for a mixed bus fleet under micro driving conditions. *IEEE Transactions on Intelligent Transportation Systems, 22*(4), 2464–2475.

Mohamed, M., Farag, H., El-Taweel, N., & Ferguson, M. (2017). Simulation of electric buses on a full transit network: Operational feasibility and grid impact analysis. *Electric Power Systems Research, 142*, 163–175.

Paul, T., & Yamada, H. (2014). Operation and charging scheduling of electric buses in a city bus route network. In *17th international ieee conference on intelligent transportation systems (itsc)* (pp. 2780–2786). IEEE.

Pelletier, S., Jabali, O., Mendoza, J. E., & Laporte, G. (2019). The electric bus fleet transition problem. *Transportation Research Part C: Emerging Technologies, 109*, 174–193.

Perumal, S. S., Dollevoet, T., Huisman, D., Lusby, R. M., Larsen, J., & Riis, M. (2021a). Solution approaches for integrated vehicle and crew scheduling with electric buses. *Computers & Operations Research, 132*, 105268.

Perumal, S. S., Lusby, R. M., & Larsen, J. (2021b). Electric bus planning & scheduling: A review of related problems and methodologies. *European Journal of Operational Research*.

Pylarinou, C., Iliopoulou, C., & Kepaptsoglou, K. (2021). Transit route network redesign under electrification: model and application. *International Journal of Transportation Science and Technology*.

Qin, N., Gusrialdi, A., Brooker, R. P., Ali, T., et al. (2016). Numerical analysis of electric bus fast charging strategies for demand charge reduction. *Transportation Research Part A: Policy and Practice, 94*, 386–396.

Ribeiro, C. C., & Soumis, F. (1994). A column generation approach to the multiple-depot vehicle scheduling problem. *Operations Research, 42*(1), 41–52.

Rinaldi, M., Picarelli, E., D'Ariano, A., & Viti, F. (2020). Mixed-fleet single-terminal bus scheduling problem: modelling, solution scheme and potential applications. *Omega, 96*, 102070.

Rogge, M., van der Hurk, E., Larsen, A., & Sauer, D. U. (2018). Electric bus fleet size and mix problem with optimization of charging infrastructure. *Applied Energy, 211*, 282–295.

Rogge, M., Wollny, S., & Sauer, D. U. (2015). Fast charging battery buses for the electrification of urban public transporta feasibility study focusing on charging infrastructure and energy storage requirements. *Energies, 8*(5), 4587–4606.

Schmid, V., & Ehmke, J. F. (2015). Integrated timetabling and vehicle scheduling with balanced departure times. *OR Spectrum, 37*(4), 903–928.

Stumpe, M., Rößler, D., Schryen, G., & Kliewer, N. (2021). Study on sensitivity of electric bus systems under simultaneous optimization of charging infrastructure and vehicle schedules. *EURO Journal on Transportation and Logistics*, 100049.

Tang, X., Lin, X., & He, F. (2019). Robust scheduling strategies of electric buses under stochastic traffic conditions. *Transportation Research Part C: Emerging Technologies, 105*, 163–182.

Teoh, L. E., Khoo, H. L., Goh, S. Y., & Chong, L. M. (2018). Scenario-based electric bus operation: A case study of putrajaya, malaysia. *International Journal of Transportation Science and Technology, 7*(1), 10–25.

Wang, C., Guo, C., & Zuo, X. (2021). Solving multi-depot electric vehicle scheduling problem by column generation and genetic algorithm. *Applied Soft Computing, 112*, 107774.

Wang, G., Li, W., Zhang, J., Ge, Y., Fu, Z., Zhang, F., … Zhang, D. (2019). Sharedcharging: Data-driven shared charging for large-scale heterogeneous electric vehicle fleets. *Proceedings of the ACM on Interactive, Mobile, Wearable and Ubiquitous Technologies, 3*(3), 1–25.

Wang, H., & Shen, J. (2007). Heuristic approaches for solving transit vehicle scheduling problem with route and fueling time constraints. *Applied Mathematics and Computation, 190*(2), 1237–1249.

Wang, J., Kang, L., & Liu, Y. (2020). Optimal scheduling for electric bus fleets based on dynamic programming approach by considering battery capacity fade. *Renewable and Sustainable Energy Reviews, 130*, 109978.

Wang, Y., Huang, Y., Xu, J., & Barclay, N. (2017). Optimal recharging scheduling for urban electric buses: A case study in davis. *Transportation Research Part E: Logistics and Transportation Review, 100*, 115–132.

Wen, M., Linde, E., Ropke, S., Mirchandani, P., & Larsen, A. (2016). An adaptive large neighborhood search heuristic for the electric vehicle scheduling problem. *Computers & Operations Research, 76*, 73–83.

Yao, E., Liu, T., Lu, T., & Yang, Y. (2020). Optimization of electric vehicle scheduling with multiple vehicle types in public transport. *Sustainable Cities and Society, 52*, 101862.

Yıldırım, Ş., & Yıldız, B. (2021). Electric bus fleet composition and scheduling. *Transportation Research Part C: Emerging Technologies, 129*, 103197.

Zhang, A., Li, T., Zheng, Y., Li, X., Abdullah, M. G., & Dong, C. (2021a). Mixed electric bus fleet scheduling problem with partial mixed-route and partial recharging. *International Journal of Sustainable Transportation*, 1–11.

Zhang, L., Wang, S., & Qu, X. (2021b). Optimal electric bus fleet scheduling considering battery degradation and non-linear charging profile. *Transportation Research Part E: Logistics and Transportation Review, 154*, 102445.

Zhou, G.-J., Xie, D.-F., Zhao, X.-M., & Lu, C. (2020). Collaborative optimization of vehicle and charging scheduling for a bus fleet mixed with electric and traditional buses. *IEEE Access, 8*, 8056–8072.

Zhu, C., & Chen, X. (2013). Optimizing battery electric bus transit vehicle scheduling with battery exchanging: Model and case study. *Procedia-Social and Behavioral Sciences, 96*, 2725–2736.